chapter 21

Tracer Kinetic Modeling

The spatial distribution of a radiotracer in the body is time varying and depends on a number of components such as tracer delivery and extraction from the vasculature, binding to cell surface receptors, diffusion or transport into cells, metabolism, washout from the tissue, and excretion from the body. Thus the temporal component often is very important in nuclear medicine studies, and the timing of the imaging relative to the administration of the radiopharmaceutical must be carefully chosen such that the images reflect the biologic process of interest. Furthermore, the rate of change of radiotracer concentration often provides direct information on the rate of a specific biologic process. This chapter discusses how the temporal information that can be obtained from nuclear medicine studies is incorporated to provide quantitative measures of physiologic parameters, biochemical rates, or specific biologic events. Further examples are provided in reference 1.

A. BASIC CONCEPTS

Dynamic nuclear medicine studies enable the radiotracer concentration to be measured as a function of time, as shown in Figure 20-10. With an understanding of the biologic fate of the radiotracer in the body, it is possible to construct mathematical models with a set of one or more parameters that can be fit to explain the observed time-activity curves. In some cases the model parameters can be related directly to physiologic or biologic quantities. Examples include tissue perfusion (measured in mL/min/g) and the rate of glucose use (measured in mol/min/g). The mathematical models that describe the time-varying distribution of radiopharmaceuticals in the body are known as *tracer kinetic models.*

Tracer kinetic models may be very simple. For example, one method for evaluating renal function is to measure the uptake of ^{99m}Tc-labeled dimercaptosuccinic acid (DMSA) using a single region of interest (ROI) positioned over each kidney at one instant in time. "Function" in this case is determined in relative rather than absolute physiologic units. A more rigorous approach for evaluating kidney function is to measure glomerular filtration rates (GFRs), in mL/min, using a tracer that is filtered by the kidneys, such as ^{99m}Tc-labeled diethylene triamine pentaacetic acid (DTPA). In this case, it is necessary to obtain serial images of the kidneys and also to collect blood samples to measure tracer concentration in the blood as a function of time. Using these data and applying an appropriate mathematical model, one can then calculate the GFR.

Each of these approaches permits an assessment of "renal function" that is based on a different model for the behavior of the kidneys. The approach of choice depends on the medical or biologic information desired, as well as on the equipment available and acceptable level of technical complexity. Developing a model requires the investigator to synthesize a large amount of biologic information into a comprehensive description of the process of interest. This chapter summarizes some of the principles and techniques in developing these models and presents some examples of tracer kinetic models currently used in nuclear medicine.

The following example illustrates the principle of tracer kinetic techniques. Figure 21-1 shows a hollow tube with a substance flowing through it. If a small amount of tracer is injected instantaneously at time t and at point A and the measured activity at point B is plotted as a function of time, the resultant time-activity curve represents a histogram of the transit times for the tracer molecules

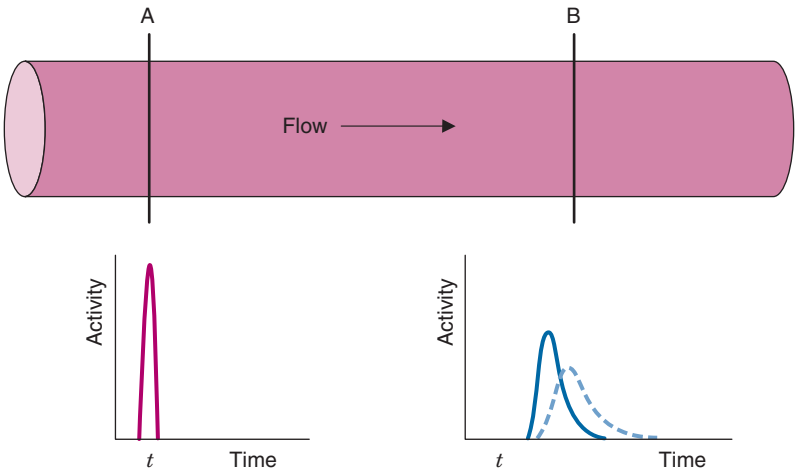

FIGURE 21-1 Illustration of use of tracer kinetics for measurement of flow. The system consists of a hollow tube characterized by flow in the direction indicated. A bolus of tracer introduced at time *t* and point A produces a time-activity curve at location B that depends on flow. Relatively higher flow (*solid line*) results in less dispersion and a shorter average transit time, whereas a lower flow rate (*dashed line*) produces a longer average transit time. (*Adapted from Phelps ME, Mazziotta JC, Schelbert HR:* Positron Emission Tomography and Autoradiography: Principles and Applications for the Brain and Heart. *New York, 1986, Raven Press.*)

from point A to point B. If the flow rate through the tube is decreased (*dashed curve* in Fig. 21-1), then the tracer molecules will on average take longer to get from point A to point B and the shape of the measured time-activity curve will change accordingly. This simple example illustrates conceptually how the kinetic information (i.e., the time-activity curve) varies in response to a change in a parameter in the system (flow rate). The flow rate, *F,* through the tube can be calculated as

$$F(\text{mL/min}) = V(\text{mL})/\tau(\text{min}) \qquad (21\text{-}1)$$

where V is the volume of the tube and τ is the mean transit time of the tracer molecules between points A and B. This is known as the *central volume principle.*

B. TRACERS AND COMPARTMENTS

Most applications of tracer kinetic principles in nuclear medicine are based on *compartmental models*. In this section, we review the basic principles of compartmental modeling.

1. Definition of a Tracer

A tracer is a substance that follows ("traces") a physiologic or biochemical process. In this chapter, tracers are assumed to be radionuclides or, more commonly, small molecules or larger biomolecules (e.g., antibodies and peptides) that are labeled with radionuclides. These labeled molecules are also known as *radiotracers* or *radiopharmaceuticals.* For simplicity, we refer to them as *tracers* in the remainder of this discussion. Tracers can be naturally occurring substances, analogs of natural substances (i.e., substances that mimic the natural substance), or compounds that interact with specific physiologic or biochemical processes in the body. Examples include diffusible tracers for blood flow, tracers that follow important metabolic pathways in cells, and tracers that bind to specific receptors on cell surfaces. Table 21-1 lists some examples of tracers that are used in nuclear medicine and their applications.

Some specific requirements for an ideal tracer include the following:

1. The behavior of the tracer should be identical or related in a known and predictable manner to that of the natural substance.
2. The mass of tracer used should not alter the underlying physiologic process being studied or should be small compared with the mass of endogenous compound being traced (a typical "rule of thumb" is that the mass of tracer should be <1% of the endogenous compound).
3. The specific activity of the tracer should be sufficiently high to permit imaging and blood or plasma activity assays without violating the first two requirements.
4. Any isotope effect (see Chapter 3, Section B) should be negligible or at least quantitatively predictable.

TABLE 21-1
SELECTED EXAMPLES OF TRACERS USED IN NUCLEAR MEDICINE

Process	Tracer
Blood flow/perfusion:	
Diffusible (not trapped)	$H_2{}^{15}O$, ^{133}Xe, ^{99m}Tc-teboroxime (heart)
Diffusible (trapped)	$^{201}TlCl$ (heart), ^{99m}Tc-sestamibi (heart), $^{13}NH_3$ (heart), $^{82}RbCl$, ^{99m}Tc-ECD (brain), ^{99m}Tc-tetrofosmin (heart), ^{62}Cu-PTSM, ^{99m}Tc-HMPAO (brain)
Nondiffusible (trapped)	^{99m}Tc-macroaggragated albumin (lung)
Blood volume	^{11}CO, ^{51}Cr-RBC, ^{99m}Tc-RBC
Ventricular function	^{99m}Tc-pertechnetate, ^{99m}Tc-DTPA
Esophageal transit time/reflux	^{99m}Tc-sulphur colloid
Gastric emptying	^{99m}Tc-sulphur colloid, ^{111}In-DTPA
Gallbladder dynamics	^{99m}Tc-disofenin, ^{99m}Tc-mebrofenin
Infection	^{111}In-WBC, ^{67}Ga-citrate, ^{99m}Tc-WBC
Lung ventilation	^{133}Xe, ^{81}Kr, ^{99m}Tc-technegas™
Metabolism:	
Oxygen	$^{15}O_2$
Oxidative	^{11}C-acetate
Glucose	^{18}F-fluorodeoxyglucose
Free fatty acids	^{11}C-palmitic acid, ^{123}I-hexadecanoic acid
Osteoblastic activity	^{99m}Tc-MDP, $^{18}F^-$
Hypoxia	^{18}F-fluoromisonidazole, ^{62}Cu-ATSM
Proliferation	^{18}F-fluorothymidine
Protein synthesis	^{11}C-leucine, ^{11}C-methionine
Receptor systems:	
Dopaminergic	^{18}F-fluoro-L-dopa, ^{11}C-raclopride, ^{18}F-fluoroethylspiperone, ^{11}C-CFT
Benzodiazepine	^{18}F-flumazenil
Opiate	^{11}C-carfentanil
Serotonergic	^{11}C-altanserin
Adrenergic	^{123}I-mIBG
Somatostatin	^{111}In-octreotide
Estrogen	^{18}F-fluoroestradiol

ATSM, diacetyl-bis (N^4-methylthiosemicarbazone); CFT, [N-methyl-^{11}C]-2-β-carbomethoxy-3-β-(4-fluorophenyl)-tropane; DOPA, 3,4-dihydroxyphenylalanine; DTPA, diethylenetriamine penta-acetic acid; ECD, ethyl cysteinate dimer; HMPAO, hexamethyl propylene amine oxime; MDP, methylene diphosphonate; mIBG, metaiodobenzylguanidine; PTSM, pyruvaldehyde bis(N^4-methylthiosemithiocarbazone); RBC, red blood cell; WBC, white blood cell.

If a tracer is labeled with an element not originally present in the compound (this is often the case with radionuclides such as ^{99m}Tc, ^{123}I, and ^{18}F), it should behave similarly to the natural substance or in a way that differs in a known manner. The strictness of this requirement depends on the process under investigation. One common use of tracers in clinical nuclear medicine is to examine gross function and distribution, including blood flow, filtration, and ventilation. Although the elements represented by radionuclides such as ^{99m}Tc, ^{67}Ga, ^{111}In, and ^{123}I are not normally present in biologic molecules, it is possible to

incorporate these radionuclides in physiologically relevant tracers that can measure simple parameters that are related to distribution, transport, and excretion.

However, these same elements are not normally present in human biochemistry (iodine is an exception when used to study thyroid metabolism). It is therefore much more difficult to mimic a biochemical reaction sequence with these radionuclides. The biochemical systems of the body are more specific than the transport processes that move or filter fluids or gases. Biochemical systems can selectively require that compounds be of one optical polarity versus the other; that compounds fit within angstroms in the cleft of an enzyme; that chemical bond angles, lengths, and strengths are appropriate; and so forth. When a compound is labeled with a foreign species, such as ^{99m}Tc, one cannot be sure that it will retain its natural properties and a careful examination and characterization of the compound must be undertaken. One of the advantages of radionuclides that represent elements normally involved in biochemical processes, such as ^{11}C, ^{13}N, and ^{15}O, is that they generally do not alter the behavior of the labeled compound.

Analog tracers are compounds that possess many of the properties of natural compounds but with differences that change the way the analog interacts with biologic systems. In many cases, analog tracers are deliberately created to simplify the analysis of a biologic system. For example, analogs that participate through only a limited number of steps in a sequence of biologic reactions have been developed in biochemistry and pharmacology. Analogs are used to decrease the number of variables that must be measured, to increase the specificity and accuracy of the measurement, or to selectively investigate a particular step in a biochemical sequence. In other cases analog tracers are used because of the need to label the tracer with an element that is not normally present in the molecule of interest. As discussed earlier, this can lead to very significant deviations in the biologic properties (particularly in small molecules) compared with the natural compound. Correction factors based on the principles of competitive substrate or enzyme kinetics are employed in studies using analog tracers to account for differences between the analog and the natural compound. A well-known and widely used example of an analog tracer in nuclear medicine is 2-deoxy-2[^{18}F]fluoro-D-glucose (FDG) to measure glucose metabolism (see Section E.5).

2. Definition of a Compartment

A *compartment* is a volume or space within which the tracer rapidly becomes uniformly distributed; that is, it contains no significant concentration gradients. In some cases, a compartment has an obvious physical interpretation, such as the intravascular blood pool, reactants and products in a chemical reaction, substances that are separated by membranes, and so forth. For other compartments, the physical interpretation may be less obvious, such as a tracer that may be metabolized or trapped by one of two different cell populations in an organ, thus defining the two populations of cells as separate compartments. Additionally, although the definition of a particular compartment may be appropriate for one tracer [e.g., the distribution of labeled red blood cells (RBCs) in the intravascular blood pool], it might not apply for a different tracer (e.g., the distribution of thallium or rubidium, which has both an intravascular and an extravascular distribution). Thus the number, interrelationship, organization, and definition of compartments in a compartmental model must be developed from knowledge of physiologic and biochemical principles.

3. Distribution Volume and Partition Coefficient

A compartment may be *closed* or *open* to a tracer. A closed compartment is one from which the tracer cannot escape, whereas an open compartment is one from which it can escape to other compartments. Whether a compartment is closed or open depends on both the compartment and the tracer. Indeed, a compartment may be open to one tracer and closed to another. If a tracer is injected into a closed compartment, such as a nondiffusible tracer in the vascular system, conservation of mass requires that after the distribution of the tracer reaches equilibrium or steady-state conditions, the amount of tracer injected, A (in becquerels or other units of activity), must equal the concentration of the tracer in the compartment, C (in Bq/mL), multiplied by the *distribution volume*, V_d, of the compartment. Thus,

$$V_d = A/C \text{ (at equilibrium)} \qquad (21\text{-}2)$$

This equation is the basis for the *dilution principle,* which provides a convenient method for determining the distribution volume of a

closed compartment, as shown by the following example.

EXAMPLE 21-1

What is the distribution volume of the RBCs if 1 MBq ^{51}Cr-labeled RBCs is injected into the blood stream and an aliquot of blood taken after an equilibration period (10 minutes) contains 0.2 kBq/mL? Assume the hematocrit, H (fraction of the total blood volume occupied by RBCs), is 0.4.

Answer

From Equation 21-2:

$$V_d = (1000 \text{ kBq})/(0.2 \text{ kBq/mL})$$
$$= 5000 \text{ mL}$$

This result gives the total distribution volume, that is, total blood volume. The RBC volume is given by

$$V_{RBC} = H \times V_d$$
$$= 0.4 \times 5000 \text{ mL}$$
$$= 2000 \text{ mL}$$

More commonly, a compartment will be open; that is, the tracer will be able to escape from it. This applies, for example, to tracers that are distributed and exchanged between blood and tissue. In this case, after the tracer reaches its equilibrium distribution,* the concentration in blood will typically be different from that in the tissue (Fig. 21-2A). The ratio of tissue concentration C_t (Bq/g) to blood concentration C_b (Bq/mL) at equilibrium, is called the *partition coefficient*, λ, defined by

$$\lambda(\text{mL/g}) = C_t(\text{Bq/g})/C_b(\text{Bq/mL}) \quad (21\text{-}3)$$

The equilibrium blood concentration, C_b, can be directly measured by taking blood samples. If one assumes that the concentration of tracer in tissue is the same as the concentration in blood (Fig. 21-2B), and applies Equation 21-2, this leads to an apparent distribution volume in tissue given by $V_1 = A_t/C_b$, in which A_t is the activity in the tissue. One also knows that $A_t = C_t \times V_t$, in which V_t is the volume (or mass) of tissue; therefore combining these relationships and Equation 21-3 yields

$$\lambda = V_1/V_t \quad (21\text{-}4)$$

Thus another interpretation of the partition coefficient is that it is the distribution volume per unit mass of tissue for a diffusible substance or tracer. This interpretation is employed in some models for estimating blood flow and perfusion, as discussed in Section E.

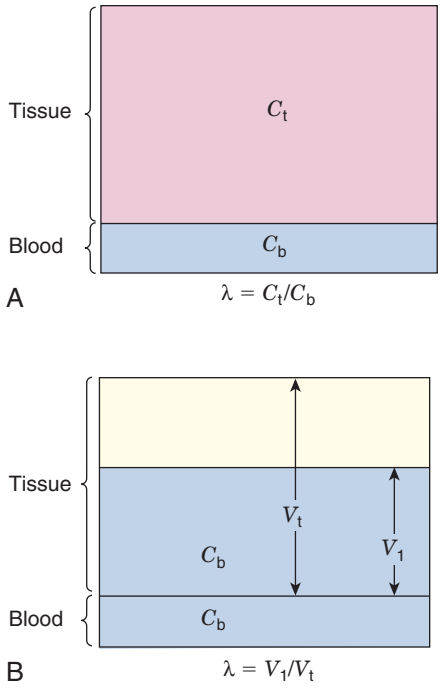

FIGURE 21-2 *A,* Partition coefficient, λ, for tracers that can diffuse or be transported into tissue from blood. The value of λ is given by the ratio of tissue-to-blood concentrations of the tracer when it has reached an equilibrium or steady-state condition. *B,* Partition coefficient also equals the ratio of the apparent distribution volume in tissue, V_1, assuming the same tracer concentration as blood-to-tissue volume (or mass), to V_t. (*From Phelps ME, Mazziotta JC, Schelbert HR:* Positron Emission Tomography and Autoradiography: Principles and Applications for the Brain and Heart. *New York, 1986, Raven Press.*)

4. Flux

Flux refers to the amount of substance that crosses a boundary or surface per unit time (e.g., mg/min or mol/min) (Fig. 21-3). It also can refer to the transport of a substance between different compartments in terms of flux per unit volume or mass of tissue (e.g., mol/min/mL or mg/min/g).

Flux is a general term that can refer to a variety of processes. For example, the total mass of RBCs moving through a blood vessel

*Note that "equilibrium" in this case means that the concentration of the tracer in the compartments has reached a constant value with time. It does not imply equilibrium in the thermodynamic sense, that is, that there is no further transport of tracer between tissue and blood. Thus tracer equilibrium is synonymous with the term *steady state* (see Section B.6).

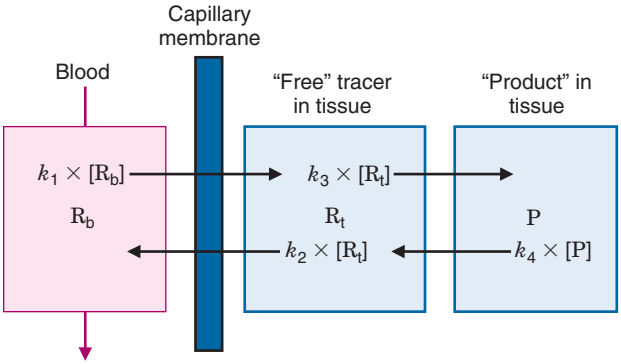

FIGURE 21-3 Three-compartment system consisting of reactants in blood (R_b) and tissue (R_t) and product in tissue (P). Fluxes between the compartments, indicated by *arrows,* are products of the first-order rate constants and the respective compartmental concentrations. (*Adapted from Phelps ME, Mazziotta JC, Schelbert HR:* Positron Emission Tomography and Autoradiography: Principles and Applications for the Brain and Heart. *New York, 1986, Raven Press.*)

per unit time is a flux. The "boundary" or "surface" in this case could be any transverse plane through the vessel. The amount of glucose moving across a cell membrane per unit time also is a flux. Fluxes therefore may either be closely related or unrelated to blood flow.

5. Rate Constants

Rate constants describe the relationships between the concentrations and fluxes of a substance between two compartments. For simple *first-order processes,* the rate constant, k, multiplied by the amount (or concentration) of a substance in a compartment determines the flux:

$$\text{flux} = k \times \text{amount of substance in compartment} \quad (21\text{-}5)$$

For first-order processes, the units of k are $(\text{time})^{-1}$. If "amount" refers to the mass of tracer in the compartment, the units of flux are mass/time (e.g., mg/min). If "amount" refers to concentration of tracer in the compartment, the units of flux are mass/time per unit of compartment volume (e.g., mg/min/mL), or mass/time per unit of compartment mass (e.g., mg/min/g). Note that, as illustrated by Figure 21-3, different directions of transport between two compartments can be characterized by different rate constants.

A first-order rate constant also may represent the fractional rate of transport of a substance from a compartment per unit time. For example, a rate constant of 0.1 min^{-1} corresponds to a transport of 10% of the substance from the compartment per minute. The inverse of the rate constant, $1/k$, is sometimes referred to as the *turnover time,* or *mean transit time*, τ, of the tracer in the compartment (in this example, 10 minutes). Similarly, the *half-time of turnover,* $t_{1/2}$, that is, the time required for the original amount of tracer in the compartment to decrease by 50% (assuming no back transfer into the compartment), is given by

$$t_{1/2} = 0.693/k \quad (21\text{-}6)$$

Thus the fractional rate constant k is analogous to the decay constant λ for radioactive decay, whereas the mean transit time is analogous to the average lifetime of a radionuclide (see Chapter 4, Section B.3). In first-order models, transport out of a compartment through a single pathway (without back-transport) is described by a single exponential function, e^{-kt}, analogous to the radioactive decay factor $e^{-\lambda t}$.

If there is more than one potential pathway for a tracer to leave a compartment, each characterized by a separate rate constant, k_i, then the turnover time of the tracer in the compartment is the inverse of the sum of all these rate constants and the half-time of turnover is

$$t_{1/2} = 0.693/(k_1 + k_2 + \ldots + k_m) \quad (21\text{-}7)$$

where m is the number of pathways by which the tracer can leave the compartment.

Most compartment models used in nuclear medicine are based on the assumption that first-order kinetics describe the dynamics of the system of interest. The tracer kinetics of such systems are linear. That is, doubling the input (amount or concentration) doubles the output (flux) of the system. As shown in Section E, linear first-order tracer kinetic models adequately describe many systems even when the dynamics of the natural substances are nonlinear.

A more general expression for the relationship among rate constants, fluxes, and concentrations (or masses) is

$$\text{flux} = k \times (\text{mass or concentration of substance})^n \quad (21\text{-}8)$$

where n refers to the *order* of the reaction. The units of rate constants for n^{th} order reactions (in terms of concentration) are [concentrations$^{(1-n)}$ • time^{-1}]. Thus only first-order rate constants represent a constant fractional turnover and Equations 21-6 and 21-7 apply only to first-order processes.

Figure 21-3 illustrates a three-compartment system consisting of a blood compartment separated by a membrane barrier (e.g., capillary wall) from two sequential tissue compartments. R and P refer to chemical reactant and product, whereas the subscripts b and t refer to reactant in blood and tissue compartments, respectively. [R_b],* [R_t], and [P] are the blood and tissue concentrations of reactant and product, whereas the fluxes between the compartments are the first-order rate constants, k_1, k_2, k_3, and k_4, multiplied by corresponding concentrations. The thicknesses of the arrows in Figure 21-3 are proportional to the magnitude of the corresponding rate constant. In this example, the rate constants into and out of tissue are larger than the corresponding rate constants between the reactant and product compartments in tissue. Thus the majority of the reactant initially transported into the tissue space is transported back into blood without undergoing any biochemical reactions. This is a common occurrence in actual biochemical systems and introduces a reserve capacity into the system that can accommodate changes in metabolic supply and demand (e.g., by changing k_3).

Figure 21-4 illustrates the relationship between first-order rate constants and the relative concentrations of the substrates in a biochemical sequence. If a substrate (S) and enzyme (E) combine to form a substrate-enzyme complex (SE), which then dissociates into a product (P) with release of the enzyme, the fluxes of the first-order reaction steps are concentrations multiplied by the corresponding rate constants. If a small amount of labeled substrate is introduced into the system at time zero, the tracer will go through the reaction steps, producing concentrations of labeled S, SE, and P as shown in the graphs in Figure 21-4. If k_3 (the forward rate constant for the reaction converting SE to E and P) is reduced by 50% with all the other rate constants remaining unchanged, the concentrations of labeled S, SE, and P are then represented by the dotted orange lines in Figure 21-4. Decreasing k_3 causes a slower production of P and causes a compensatory increase in labeled S and SE.

6. Steady State

The term *steady state* refers to a condition in which a process, parameter, or variable is not changing with time. For example, a flux through a biochemical pathway is said to be in a steady state when the concentration of reactants and products are not changing with time. In all tracer kinetic models, it is assumed that the underlying process that is being measured

*The notation [X] is used to denote the concentration (usually in units of g/mL or mol/mL) of substance X.

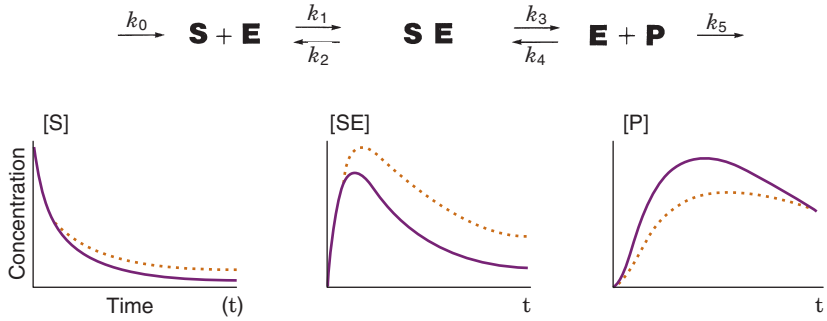

FIGURE 21-4 Illustration of tracer kinetics of a chemical reaction sequence. First-order rate constants (k_0, k_1, k_2, k_3, k_4, k_5) characterize the various reaction steps, whereas S refers to substrate, E refers to enzyme, P is product, and SE is the substrate-enzyme complex. The time-activity relationships for concentrations of labeled S, SE, and P are shown for a particular value of k_3 (*solid purple line*) and with k_3 reduced by 50% (*dotted orange line*). (*From Phelps ME, Mazziotta JC, Schelbert HR:* Positron Emission Tomography and Autoradiography: Principles and Applications for the Brain and Heart. *New York, 1986, Raven Press.*)

by the tracer is in a steady state. Because of biorhythms, steady states almost never exist in the body; however, if the magnitude or temporal period of change is small compared with the process being measured, then the steady-state assumption is reasonable. In many cases, the experimental sampling rate is slow compared with the biorhythm (e.g., blood sampling rate vs. pulsatile nature of blood flow) and it is not perceived in the measured data. In these cases, the measured parameters represent average values of the function measured. However, if the experimental sampling rate is fast compared with the biorhythm, significant errors can be introduced in the model calculations. In this case, the calculated parameters typically do not represent a simple average of the non-steady-state values.

Steady state of a process should not be confused with steady state of the tracer. Measurements of the tracer commonly are made when the tracer itself is not in steady state but rather while it is distributing through the process under study. Some tracer kinetic models are used in which measurements are made when both the tracer and process studied are in a steady state. These methods usually are referred to as "equilibrium" models.

An important and useful property of a steady-state condition is that the rates (fluxes) of all steps in a nonbranching transport or reaction sequence are equal. Thus if a tracer technique is used to measure one step in a sequence, the rate for each step in the entire sequence can be determined. If the reaction branches into two or more separate pathways then the sum of each pathway must equal the rate of the preceding step. In this case, if one determines the rate of any of the preceding steps and also knows the branching fractions, then the rate of each branch can be determined by multiplying the rate of the preceding step by the branching fraction. For example, if the reaction sequence in Figure 21-5 is in a steady state and the rate of disappearance of A is R_A, the rates of formation of B, C, D, and E are R_B, R_C, R_D, and R_E, respectively, and f_d and f_e are the branching fraction down the corresponding pathways, then

$$R_A = R_B = R_C = (R_D + R_E) \qquad (21\text{-}9)$$

and

$$R_D = f_D \times R_C \qquad (21\text{-}10)$$

$$R_E = f_E \times R_C \qquad (21\text{-}11)$$

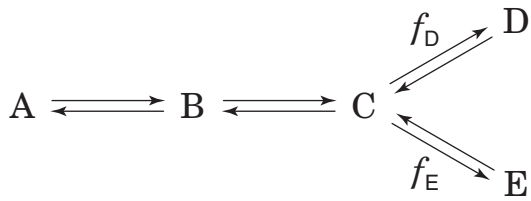

FIGURE 21-5 Example of a multistep reaction sequence that branches into two pathways. The terms f_D and f_E are the branching fractions for the corresponding pathways ($f_D + f_E = 1$).

where

$$f_D + f_E = 1 \qquad (21\text{-}12)$$

C. TRACER DELIVERY AND TRANSPORT

A tracer that is injected into the body must follow several steps in sequence before it can enter a biochemical pathway: delivery to the capillary via blood flow, extraction across the capillary wall into the tissue space, and finally, incorporation into a biochemical reaction sequence. Although only one of the steps in a process may be of interest in a particular application, it may be influenced by other steps in the process of tracer delivery. In this section we examine tracer techniques for describing these processes.

1. Blood Flow, Extraction, and Clearance

Blood flow through vessels is described in units of volume per unit time (usually in units of mL/min). For regional tissue measurements it is blood flow per mass of tissue that is determined (mL/min/g). Blood flow per mass of tissue is more properly referred to as *perfusion*; however, in the literature the term *blood flow* is used to indicate both blood flow and blood flow per mass of tissue. In both cases the basic phenomenon is still blood flow. Thus relationships involving blood flow apply equally to blood flow and perfusion, provided that care is taken to ensure that the units are consistent. For example, in the relationship between blood flow and blood volume (see Section E.4), if blood flow is in units of mL/min, then blood volume must be in units of mL. If blood flow is in units of mL/min/g, then blood volume must be in units of volume per mass of tissue (mL/g). In this text, the

term *blood flow,* symbolized by *F,* is used to denote either blood flow or blood flow per mass of tissue. The units indicate which quantity is being discussed.

In addition to its dependence on blood flow, the uptake of a tracer by tissue depends on tissue extraction and clearance. Extraction is defined in two different contexts: net and unidirectional. *Net extraction* refers to the difference in steady-state tracer concentrations between the input and output blood flow of an organ. If the input (arterial) concentration is C_A, and the output (venous) concentration is C_V, the net extraction fraction, E_n, is defined as

$$E_n = (C_A - C_V)/C_A \qquad (21\text{-}13)$$

If there is no metabolism of the tracer, that is, if all the tracer delivered to the tissue eventually is returned to the blood, the net extraction is zero. This situation applies, for example, to inert diffusible blood flow tracers when steady-state conditions for the tracer are reached.

Unidirectional extraction refers to the amount of tracer extracted only from blood to tissue. It does not include the amount transferred back from tissue to blood. Thus the unidirectional extraction fraction, E_u, generally is larger than the net extraction fraction. An exception to this general rule occurs with O_2. Virtually all oxygen extracted by tissue is metabolized; thus the net and unidirectional extraction fractions are the same. For essentially all other substances, a major portion of what is extracted by the tissue is transported back to blood. This is the situation represented by the bidirectional transport in the model shown in Figure 21-3.

Extraction fractions are expressed as fractions or as percentages and can be measured using tracer kinetic techniques. To determine net extraction, it is necessary to measure the input and output concentrations of the tracer in the blood under steady-state conditions, that is, after the concentrations have reached constant values. The route of administration of the tracer is unimportant in this case. For example, the tracer can be administered by constant infusion or as a bolus into a peripheral vein.

Unidirectional extraction can be measured by observing the rate of uptake by the tissue or organ immediately after injection of the tracer, that is, when the blood concentration is maximum and the tissue concentration is zero. Measurements of unidirectional extraction are useful for studying the transport properties of substrates and drugs.

An important concept relating the processes of blood flow, flux, and extraction is the *Fick principle.* This principle is based on the conservation of mass and states that, under steady-state conditions, the net uptake of a tracer (or other substance) is simply the difference between the input to and output from the organ or tissue. If the input (arterial) concentration of the tracer is C_A (mg/mL) and the output (venous) concentration is C_V (mg/mL), and the blood flow to the organ is F (mL/min), then the net uptake rate, U (mg/min), is given by

$$U = F \times (C_A - C_V) \qquad (21\text{-}14)$$

As an example, if the arterial and venous concentrations of oxygen and the blood flow to an organ are measured, Equation 21-14 can be used to determine the oxygen utilization rate for that organ. If blood flow F in Equation 21-14 is replaced by blood flow per mass of tissue (perfusion), then the uptake or utilization is given in units of utilization per mass of tissue (mg/min/g).

The Fick principle can be employed only under steady-state conditions. An alternative approach that is applicable to non–steady-state conditions is the Kety-Schmidt method, which is discussed in Section E.4.

The extraction of tracers generally occurs across membranes or through the fenestrations* found in capillaries. The extraction fraction of a tracer depends on the capillary surface area, S, the capillary permeability for the tracer, P, and blood flow through the capillaries, F. A simple model relating these quantities was developed by Renkin[2] and Crone.[3] Figure 21-6 illustrates an idealized capillary

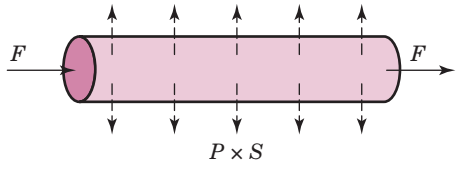

FIGURE 21-6 Renkin-Crone capillary model. The capillary is assumed to be a rigid tube, and extraction from blood to tissue is characterized by the product of the permeability, P, and surface area, S. Blood flow through the capillary is F.

*Fenestrations are small gaps found between the junctions of cells in the capillary wall.

(i.e., rigid tube) through which is passing a tracer with flow *F*. It is assumed that the concentration of tracer across the cross-section of the capillary at any point along its length is constant and that the extraction of tracer from the capillary to the tissue at any point is proportional to the concentration of the tracer in the blood. It is further assumed that extraction is unidirectional; that is, there is no back-transfer of the tracer from tissue to blood.

For this simple model, it can be shown that the unidirectional extraction fraction E_u for the capillary is given by

$$E_u = 1 - e^{-(P \times S/F)} \qquad (21\text{-}15)$$

Thus the extraction fraction depends only on the permeability-surface area product, $P \times S$ (mL/min), and on flow, *F*. This equation also can be stated in terms of perfusion, by replacing blood flow with perfusion (mL/min/g) and the permeability-surface area product with $P \times S$ for a capillary network per mass of tissue (mL/min/g).

EXAMPLE 21-2

What is the unidirectional extraction fraction for the diffusible tracer $^{13}NH_3$ in the brain if $P \times S = 0.25$ mL/min/g and blood flow to the brain (perfusion) is 0.50 mL/min/g?

Answer

From Equation 21-15:

$$E_u = 1 - e^{-(0.25/0.50)} = 0.39$$

The Renkin-Crone model is not completely realistic, because it assumes no back-transfer of tracer from tissue to blood, that the permeability-surface area product, $P \times S$, does not depend on blood flow, and that the capillary is a rigid tube. Nevertheless, it is instructive for illustrating the relationships between extraction fraction, blood flow, and the permeability-surface area product.

The ratio $[(P \times S)/F]$ sometimes is referred to as the *extraction coefficient*. One interpretation of the product, $P \times S$, is that it represents the flow of the tracer from blood to tissue through the capillary wall, whereas *F* represents flow through the capillary itself. These two "flows" represent competing processes for removal of the tracer from the capillary. Thus the fraction of a substance that is extracted by tissue can be increased either by increasing the flow through the capillary wall, $P \times S$, or decreasing the blood flow through the capillary. For a given value of $P \times S$, the greater the flow, *F*, the shorter the residence time of the tracer in the capillary, and, thus, the less the chance that the tracer will escape through the capillary wall. This is illustrated graphically in Figure 21-7.

On the other hand, the *amount* of material entering the tissue depends on the product of blood flow times extraction fraction, $F \times E$. This product is sometimes referred to as *clearance* and has the same units as flow (i.e., mL/min or mL/min/g). In essence, it represents "virtual flow" from the capillary into the tissue. Typically the increased amount of tracer that is delivered to the capillary with increasing blood flow more than offsets the decrease in the extraction fraction, with the net result that clearance increases with flow. This is illustrated graphically in Figure 21-8. Note that for small values of $P \times S$, that is, low flow across the capillary membrane, clearance is low and reaches a plateau value for relatively low values of capillary blood flow, *F*, whereas for large values of $P \times S$, clearance continues to increase with increasing flow through the capillaries. This indicates that the clearance or deposition of a tracer into tissue will have a high or low dependence on blood flow, depending on whether it has a high or low value of $P \times S$.

Clearance of tracers from tissue to blood also is used in tracer kinetic modeling. The most common use of tissue-to-blood clearance is in the measurement of bidirectional transport and blood flow.

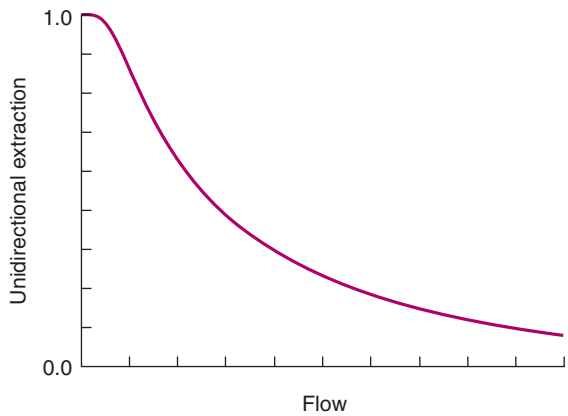

FIGURE 21-7 Unidirectional extraction fraction versus flow for the Renkin-Crone model. The extraction fraction is 1 when flow is near zero and decreases toward zero as flow increases.

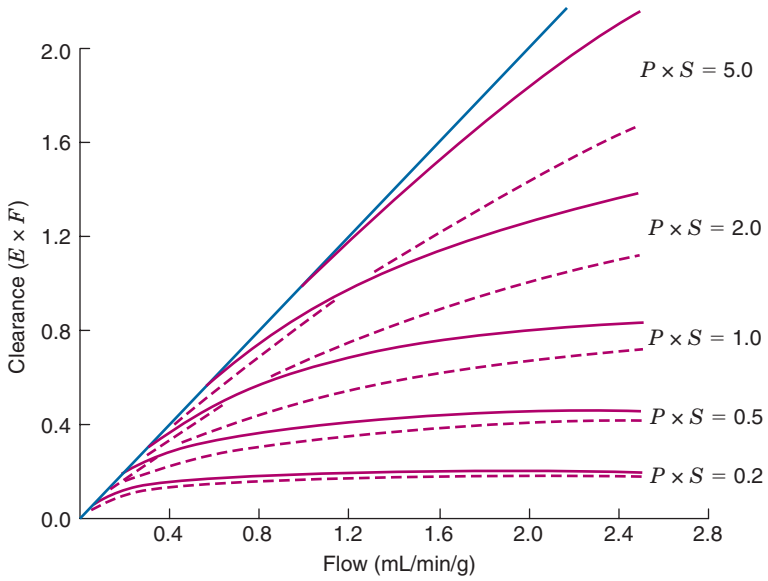

FIGURE 21-8 Clearance (flow × unidirectional extraction fraction) versus flow for various values of the permeability-surface area product, $P \times S$, for the Renkin-Crone model (*solid red lines,* Equation 21-15) and for a compartmental model description (*dashed red lines,* Equation 21-20). $P \times S$ is in units of mL/min/g. The *solid blue line* corresponds to the situation where E=1. (*From Phelps ME, Mazziotta JC, Schelbert HR:* Positron Emission Tomography and Autoradiography: Principles and Applications for the Brain and Heart. *New York, 1986, Raven Press.*)

2. Transport

Three different mechanisms exist for the transport of substances across a membrane or capillary wall. *Active* transport mechanisms require energy and can move substances against concentration gradients. Usually the energy source is adenosine triphosphate. Examples of active transport are the sodium-potassium "pump" that maintains the difference between intracellular and extracellular concentrations of these ions and the renal tubular reabsorption of glucose.

Passive transport mechanisms do not require energy and move substances in the same direction as the concentration gradient. The passive mechanisms include *carrier-mediated* diffusion, such as glucose and amino acid transport from blood to brain, and *passive* diffusion, which depends only on the existence of a concentration gradient, such as the diffusion of ^{99m}Tc-pertechnetate from blood to brain through a disrupted blood-brain barrier. Bulk flow across fenestrations in capillaries also accounts for a fraction of passive transport but varies from tissue to tissue; for example, it is insignificant in the brain when the blood-brain barrier is intact, but it is a major source of capillary/tissue transport in the heart.

Simple passive diffusion for a given membrane and molecule is characterized by a *diffusion constant, D*. Membrane permeability is related to the diffusion constant by

$$P\ (\text{cm/min}) = D\ (\text{cm}^2/\text{min})/x\ (\text{cm}) \qquad (21\text{-}16)$$

where x is the thickness of the membrane or the diffusion path length. One usually deals with the $P \times S$ product rather than P itself because in most applications the regional capillary surface area S is not known accurately. The larger the value of D (or $P \times S$), the more rapid the passive diffusion process and the greater the clearance of the substance from blood to tissue or from tissue to blood (Fig. 21-8). Many substances and in vivo processes depend on passive diffusion mechanisms, such as water, oxygen, ammonia, and carbon dioxide.

Carrier-mediated diffusion is somewhat more complicated. It also transports substances in the same direction of a concentration gradient and is characterized by the following reaction process:

$$\text{S} + \text{C} \underset{k_2}{\overset{k_1}{\rightleftarrows}} \text{SC} \underset{k_4}{\overset{k_3}{\rightleftarrows}} \text{C} + \text{S} \qquad (21\text{-}17)$$

where S is the substrate and C is the carrier molecule. SC is a carrier/substrate complex that physically moves across the membrane and then dissociates into C and S, and k_1, k_2, k_3, and k_4 are first-order rate constants that

characterize the respective steps of the process. Because only a finite number of carrier molecules are available, this type of transport process can be saturated. The rate of the process increases as the substrate concentration S increases, but only to the point of saturating the number of available carrier sites. Generally, the carrier C is a protein enzyme that is neither created nor destroyed in the reaction but only enhances its rate. The kinetics of carrier-mediated diffusion are described further in Section E.5.

D. FORMULATION OF A COMPARTMENTAL MODEL

Most models commonly in use in nuclear medicine are compartmental models with first-order rate constants describing the flux of material between compartments. Consider the simple two-compartment model illustrated in Figure 21-9. If a tracer is present in compartment A with concentration defined by $C_A(t)$ (e.g., a tracer administered as a bolus injection so that the concentration in A is time dependent), then the rate of change in concentration of compartment B [i.e., $dC_B(t)/dt$] is described by

$$dC_B(t)/dt = \text{flux into B} - \text{flux out of B} \quad (21\text{-}18)$$

Because first-order kinetics apply, the flux into B is simply $k_1C_A(t)$ and the flux out of B is $k_2C_B(t)$; therefore

$$dC_B(t)/dt = k_1C_A(t) - k_2C_B(t) \quad (21\text{-}19)$$

This first-order ordinary differential equation with constant coefficients is a typical, although simple, example of the equations necessary to mathematically define a tracer kinetic model. The time course of the tracer in the delivery compartment (usually the blood) [$C_A(t)$] is known as the *input function,* whereas the rate constants k_1 and k_2 are model parameters.

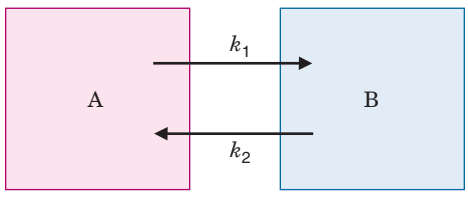

FIGURE 21-9 Transport between two compartments, A and B, is described by rate constants k_1 and k_2.

Typically, compartment A would represent the vascular compartment and compartment B might represent the amount of tracer present in the tissue. The parameters k_1 and k_2 can be estimated numerically with a technique known as *regression analysis.* The input function $C_A(t)$ is directly measured from blood samples or images of the blood (typically the left ventricular blood pool is chosen because of its large size), and the time course of activity in tissue $C_B(t)$ is determined from a time sequence of nuclear medicine images (see Fig. 20-10) or other counting measurements. A detailed discussion of regression analysis and other numerical methods related to tracer kinetic models is beyond the scope of this chapter, and the interested reader is referred to reference 1 for further details (see also Chapter 9, Section E.4).

The simple compartmental model illustrated in Figure 21-10 also can be used to describe the relationship between extraction and blood flow discussed in Section C.1 in reference to the Renkin-Crone model (Equation 21-15). In the compartmental model, the vascular space in the capillary is assumed to be a compartment of uniform concentration. The extraction and venous blood flow compete through the common vascular pool for removal of tracers. According to this compartmental model, the extraction E is related to flow F and the $P \times S$ product as:

$$E = (P \times S)/[(P \times S) + F] \quad (21\text{-}20)$$

Tissue extraction as a function of blood flow for this compartmental model is illustrated by the *dashed red lines* in Figure 21-8. The amount of extraction predicted with the compartmental model is lower than that predicted with the Renkin-Crone model for a given $P \times S$ value. In addition, the change in extraction with blood flow is somewhat different. In most

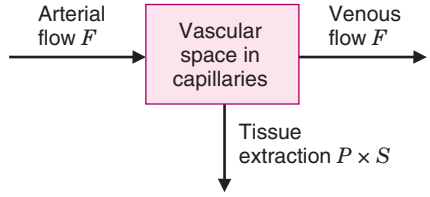

FIGURE 21-10 Compartmental model of capillary in which tissue extraction is competing with the venous flow for the tracer that is delivered by the arterial blood flow. (*From Phelps ME, Mazziotta JC, Schelbert HR:* Positron Emission Tomography and Autoradiography: Principles and Applications for the Brain and Heart. *New York, 1986, Raven Press.*)

modeling applications of interest in nuclear medicine, the Renkin-Crone model (Equation 21-15) and the compartmental model (Equation 21-20) of capillary extraction yield substantially equivalent results.

In nuclear medicine studies, there generally are two sources of data that can serve as input to a tracer kinetic model: the time course of the injected radiotracer in whole blood or plasma (the *input function*), and the measured amount of activity in tissue (the *tissue response*), usually obtained from ROI analysis of a dynamic series of images. The ROI count values are equivalent to local tissue concentrations of the tracer of interest if appropriate corrections are made for attenuation and other causes of counting inaccuracy. Additionally, the devices used to measure radioactivity in blood and tissue (e.g., a well counter and a gamma camera) must be calibrated so corrections can be made to account for their differences in counting efficiencies.

Figure 21-11 illustrates the relationships between input function and tissue response curves for two different models and two different input functions. The curves for the first model (a three-compartment model with three rate constants) illustrate how the shape of the tissue response curve changes as the shape of the input function changes. In both cases, the kinetics of the tracer in tissue are identical, but the temporal response in tissue is influenced by the input function (e.g., changing the rate of injection could produce this pattern). The parameters of the model (the rate constants) are unchanged in these two situations. If one did not measure the input function in this example and measured only the tissue response function, the different tissue response functions might be interpreted incorrectly as a change in the rate of the physiologic or biochemical process in the tissue.

The second example (bottom row of Figure 21-11), shows a four-compartment model representing a more-complicated biological process. This model produces a different tissue response when presented with the same input function as the first example.

Thus Figure 21-11 shows that the shape of the tissue response is a function of both the input function and a characteristic of the tissue "system" called the *impulse response.*

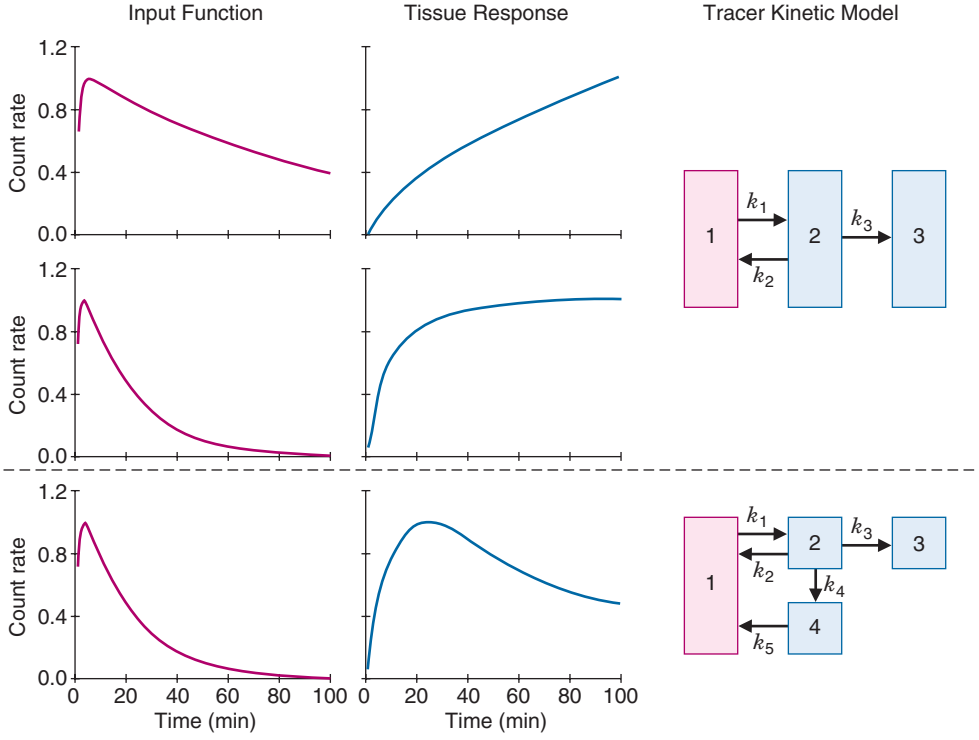

FIGURE 21-11 Input function and tissue response (sum of the tracer concentration in tissue) for two different models and for two different shapes of input functions. Different input functions produce different tissue responses for a given model configuration (*top two rows*), whereas the same input function produces different tissue responses for two different model configurations (*bottom two rows*). (*From Phelps ME, Mazziotta JC, Schelbert HR:* Positron Emission Tomography and Autoradiography: Principles and Applications for the Brain and Heart. *New York, 1986, Raven Press.*)

The impulse response of a linear system is the system's response when presented with an impulse as an input function. An impulse is in essence a function of infinitely short duration with an undefined magnitude at the origin and that has an integrated value of one if summed over all time. It can be thought of as an "idealized bolus" input given instantaneously (i.e., beyond zero time it has a zero value). In reality, a practical "impulse" delivery of tracer to a system has a duration shorter than the shortest vascular transit time through the organ. In this case there is no significant clearance of the tracer from the organ until after all the tracer has been delivered.

E. EXAMPLES OF DYNAMIC IMAGING AND TRACER KINETIC MODELS

In this section we show examples of the use of dynamic imaging and tracer kinetic models that are relatively simple and instructive. In research applications of nuclear medicine, a wide variety of more complex models are employed that are beyond the scope of this text. In many cases, there is considerable debate over the exact formulation of these complex models and the interpretation of the model parameters. Research in this area is of continued importance, particularly with the ongoing development of new radiotracers.

1. Cardiac Function and Ejection Fraction

^{99m}Tc-labeled RBCs are used for dynamic (first-pass) and equilibrium-gated studies of the heart. If a bolus of ^{99m}Tc-labeled RBCs is injected intravenously and their distribution through the thorax as a function of time is imaged dynamically with a gamma camera, the images will show the flow of blood through the venous system into the right atrium and right ventricle, to the lungs, and then to the left atrium, left ventricle, and out through the aorta to the systemic circulation. Abnormalities in this flow pattern (such as those produced by structural defects in the heart that cause intracardiac shunts) result in an abnormal distribution of the bolus of activity. For example, a ventricular septal defect with shunting of blood from the right to the left ventricle will result in an early appearance of the bolus of activity in the left ventricle as some of the blood (and labeled RBCs) bypasses the lungs and travels directly to the left ventricle. The amount of shunting can be estimated if time-activity curves of the radiotracer distribution are generated and an appropriate model is applied.

Once the RBCs have distributed uniformly throughout the vascular system (i.e., equilibrium is reached), the gamma camera images will reflect regional blood volume. If the distribution of activity over the left ventricle is plotted as a function of time by gating the acquisition to the electrocardiogram signal, changes in ventricular volume caused by cardiac contractions can be seen (Fig. 21-12). This permits calculation of the ventricular ejection fraction (EF) because the relative number of counts within the ventricle is proportional to the blood volume of the ventricle (see Section B.3).

EXAMPLE 21-3

^{99m}Tc-labeled RBCs are injected intravenously and the number of counts within the left ventricle are plotted as a function of time (Fig. 21-12) after the labeled RBCs have equilibrated within the blood pool. Calculate the left ventricular EF using the data shown.

Answer

The EF is defined as the difference between the end-diastolic volume (EDV) and the end-systolic volume (ESV) divided by EDV. Therefore,

$$\begin{aligned} EF &= (EDV - ESV)/EDV \\ &= (13 - 7)/13 \\ &= 46\% \end{aligned}$$

2. Blood Flow Models

Many tracer kinetic methods and models to measure blood flow exist. Virtually all such methods are included in one of three

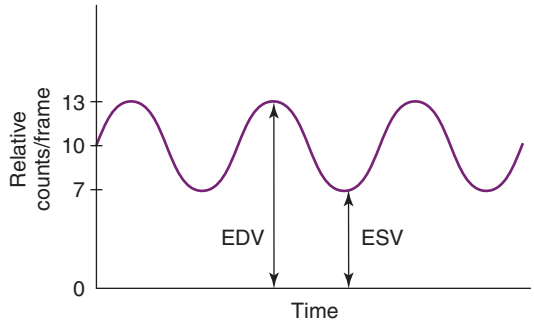

FIGURE 21-12 Sinusoidal curve illustrating relative counts per frame in a gated blood-pool image. The counts measured at the peaks and troughs of the curve are proportional to end-diastolic volume (EDV) and end-systolic volume (ESV), respectively.

categories: trapping, clearance, and equilibrium techniques. These techniques can be implemented by administering compounds labeled with either gamma-emitting or positron-emitting isotopes and imaging their distribution with gamma cameras, single-photon emission computed tomography (SPECT), or positron emission tomography (PET) scanners (see Table 21-1). All three techniques require measuring the concentration of tracer in arterial blood if quantitative estimates of blood flow in units of mL/min or mL/min/g (perfusion) are desired.

In *trapping* methods, tracers are used that are distributed to organs in proportion to blood flow but that are then trapped, either physically in the circulation (e.g., trapping of macroaggregated albumin labeled with ^{99m}Tc in the pulmonary capillaries in lung perfusion studies), or metabolically in tissue (e.g., $^{13}NH_3$ and ^{99m}Tc-sestamibi).

Clearance methods require injecting metabolically inert labeled tracers that also are distributed in proportion to flow but that do not remain trapped in the vascular or tissue spaces. The rate of washout, or clearance, of these tracers depends on blood flow. Either nondiffusible tracers that remain within the vascular compartment or diffusible tracers that distribute in both the tissue and vascular compartments can be used. As discussed later, with both classes of tracers, the mathematical approach to measuring blood flow is similar.

Equilibrium techniques require administering a continuous supply of a diffusible blood flow tracer, waiting until a tracer steady state has been reached, and then imaging the distribution. This approach uses very short half-life radionuclides such as ^{15}O ($T_{1/2}$ = 122 seconds) in which equilibrium is established by removal of the tracer from tissue by the rate of blood flow and the rate of radioactive decay. This method is not commonly used and is not discussed further here.

3. Blood Flow: Trapped Radiotracers

A simple trapping method for measuring blood flow employing nondiffusible tracers is the *labeled microsphere* technique. Microspheres are spherical or irregularly shaped small particles that are larger than capillaries and embolize (become lodged in) the first capillary bed they encounter. They remain within the capillary system for a time that is sufficiently long so that particle breakdown and excretion are insignificant during the measurement period.

If labeled microspheres are injected into the left atrium or ventricle, they are distributed to individual organs in proportion to the blood flow to the organ. If the total activity of microspheres injected is A_t, blood flow to an organ can be calculated from

$$F(\text{mL/min}) = C.O.(\text{mL/min}) \times (A_o/A_t) \quad (21\text{-}21)$$

where A_o is the activity of microspheres accumulated in the organ (assuming 100% are trapped) and *C.O.* is the cardiac output (mL of blood per minute). A_o is determined by tissue sampling or from quantitative imaging measurements. Cardiac output must be measured independently as described later. Organ perfusion, that is, blood flow per gram of tissue, is then given by

$$F(\text{mL/min/g}) = C.O. \times [(A_o/m_o)A_t] \quad (21\text{-}22)$$

where A_o/m_o is the concentration of activity in the organ or the measured tissue sample.

If the labeled microspheres are not 100% trapped, A_o will be reduced and Equations 21-21 and 21-22 will lead to underestimations of flow or organ perfusion. This effect is illustrated graphically in Figure 21-8 for tracers with a $P \times S$ product below the value required for 100% clearance over the blood flow range studied.

Frequently, cardiac output is difficult to measure. In such cases, flow to a single organ can be determined by a modification of the method just described, known as the *reference sample technique*. In this technique, arterial blood is withdrawn at a rate S (mL/min) during the time when the microspheres are flowing to the organ, and the total activity of the blood sample withdrawn, A_s, is determined. Blood flow to the organ then is calculated from

$$F = S(\text{mL/min}) \times (A_o/A_s) \quad (21\text{-}23)$$

where A_o is the activity of microspheres trapped in the organ. *Perfusion* of blood into the organ is calculated from

$$F = S \times [(A_o/m_o)/A_s] \quad (21\text{-}24)$$

Although the microsphere technique is conceptually simple, it requires injection of the tracer into the left atrium (rather than intravenously) to avoid extraction of particles by the lungs. This technique also causes

microembolization of capillaries exposed to the particles, blocking blood flow through those capillaries. To minimize perturbation of the system being studied, only a small number of microspheres are injected. An example of the labeled microsphere technique is the use of labeled albumin (which dissolves with time) to determine lung perfusion or to detect right-to-left cardiac shunts. The microsphere technique is used infrequently in humans but is quite commonly used in research studies involving animals.

More commonly, diffusible tracers that do not remain within the vascular space and that are trapped in tissue are used to trace and quantitate blood flow in human studies. Indeed, all tracers injected into the vascular system initially behave as "blood flow tracers" to some degree, but not all tracers permit convenient quantitation of blood flow independent of other processes such as extraction, metabolism, and so forth. A good diffusible tracer used to estimate blood flow by the trapping method must have high first-pass extraction into the tissue (Equation 21-15) so that tissue uptake reflects blood flow. It must also be rapidly trapped in tissue, minimizing the amount of tracer that can be transported back out of the tissue and into the blood. Examples of diffusible tracers that are trapped in tissue in proportion to blood flow include ^{99m}Tc-sestamibi, $^{13}NH_3$, ^{62}Cu-PTSM, ^{201}TlCl, and ^{82}RbCl. Blood flow can be estimated using Equation 21-24 as long as a reference arterial blood sample is available.

EXAMPLE 21-4

Suppose that microspheres are labeled with a radionuclide that permits quantitative measurement of concentrations in tissues (e.g., ^{18}F measured by PET). For simplicity, assume that these measurements can be related to the actual number of microspheres present. Calculate blood flow per gram of tissue (i.e., perfusion) to the brain if 500,000 microspheres are injected into the left atrium, and the average concentration of microspheres measured in the brain is 50 microspheres/g. Assume the cardiac output is 5 L/min.

Answer

From Equation 21-22, blood flow per gram of tissue is given by

$$F = \frac{5000(\text{mL/min}) \times 50(\text{microspheres/g})}{500{,}000 \text{ microspheres}}$$
$$= 0.50 \text{ mL/min/g}$$

EXAMPLE 21-5

Assume in the situation of Example 21-4 that the cardiac output is unknown. After injecting 500,000 microspheres into the left atrium, arterial blood is sampled at a rate of 10 mL/min. The average microsphere concentration in the whole brain is again 50 microspheres per gram. Assume the microspheres are 100% trapped in capillaries in one pass through the circulation (e.g., in 1 minute). A total of 1000 microspheres are counted in the radial arterial sample obtained in a 1-minute period. What is the average brain blood flow per gram of tissue?

Answer

From Equation 21-24:

$$F = \frac{10 \text{ (mL/min)} \times 50 \text{ (microspheres/g)}}{1{,}000 \text{ microspheres}}$$
$$= 0.50 \text{ mL/min/g}$$

4. Blood Flow: Clearance Techniques

Most clearance techniques for measuring blood flow are based on the *central volume principle,* which was defined in Equation 21-1. In the case of blood flow in units of mL/min, V is in units of mL. For blood flow in units of mL/min/g, V is in units of mL/g (volume per mass of tissue).

For a nondiffusible tracer, that is, one that stays within the vascular space, V is the blood volume in mL or mL/g, depending upon the units of blood flow. The determination of F with a nondiffusible tracer requires the measurement of both the transit time, τ, and V. Normally, with nondiffusible tracers only τ is measured, which thus provides a measure of F/V. Because F changes with both τ (τ decreases as F increases) and V (V increases as F increases), there is a nonlinear relationship between F/V and τ, with the magnitude of changes in τ being less than the magnitude of changes in F.

It is more common and easier to measure blood flow with freely diffusible tracers. Freely diffusible tracers are those that have 100% extraction from blood to tissue during a single transit through the vascular bed of the tissue. Extraction occurs almost exclusively at the level of capillaries because of their large vascular surface area. If the tracer is chemically inert, it will be cleared from tissue in proportion to blood flow and F can be determined by

Equation 21-1. For diffusible tracers, V is the volume into which the tracer is distributed. The fraction of the total tissue that a diffusible tracer will occupy depends on the specific diffusion and solubility properties of the tracer. This volume is denoted by V_1, as described in Section B.3. Thus, by substituting V_1 for V in Equation 21-1 and rearranging,

$$F/V_1 = 1/\tau \tag{21-25}$$

Multiplying each side of Equation 21-25 by V_1/V_t, in which V_t is the total tissue volume, gives

$$\begin{aligned}(F/V_1)(V_1/V_t) &= (1/\tau)(V_1/V_t)\\ F/V_t &= \lambda/\tau\end{aligned} \tag{21-26}$$

where V_1/V_t is the partition coefficient (λ) for the tracer as given by Equation 21-4. As discussed earlier, λ typically is measured using Equation 21-3. F/V_t is blood flow per volume or mass of tissue (perfusion). As discussed in Section B.1, by convention in the literature F/V_t is also referred to as blood flow, F. Thus Equation 21-26 also may be written as $F = \lambda/\tau$.

The problem of V varying with flow, discussed earlier for nondiffusible tracers, does not exist to any significant degree with diffusible tracers. The term V with diffusible tracers is the tissue volume that does not change appreciably with changes in blood flow. Thus changes in $1/\tau$ are directly proportional to flow. In addition, τ is longer for diffusible tracers (i.e., 30 to 100 seconds for brain) than for nondiffusible tracers (3 to 6 seconds for brain). Because of the longer values of τ and the linear relationship between τ and blood flow with diffusible tracers, they usually provide more accurate and convenient measurements of blood flow than those obtained with nondiffusible tracers. However, λ usually is measured in normal tissue, and it may vary from this value in pathologic tissues. For example, ^{15}O-labeled water has little variability,[1] whereas ^{133}Xe has considerable variability[4] between normal and diseased tissue.

An example of the application of the central volume principle is the *Kety-Schmidt method* for measuring cerebral blood flow with inhaled, diffusible, inert gasses (e.g., nitrous oxide or krypton).[5] This approach is based on the assumption of a constant partition coefficient of 1 mL/g in the case of nitrous oxide and krypton in the brain. Blood flow is given by (Equation 21-26)

$$\begin{aligned}F &= \lambda/\tau = 1.0\ \text{mL/g/}\tau\ (\text{min})\\ &= \tau^{-1}\ (\text{mL/min/g})\end{aligned} \tag{21-27}$$

The technique thus requires measuring the mean transit time of the gas through the brain. The original technique involved giving a subject a continuous inhalation of the gas and sampling the gas concentrations in the arterial supply to the brain (i.e., any convenient arterial source) and the venous drainage (internal jugular bulb). Gas was breathed until an equilibrium (or near equilibrium) concentration was reached in the brain and blood. The law of conservation of mass (Fick principle, Equation 21-14) states that the total amount of tracer in the brain at equilibrium must be the difference between the cumulative input and output. Therefore

$$V \times C_E = F\int_0^\infty C_A(t)dt - F\int_0^\infty C_V(t)dt \tag{21-28}$$

But $\lambda/F = \tau$ (Equation 21-26); therefore rearranging Equation 21-28 and writing it in terms of blood flow per volume of tissue

$$\frac{\lambda}{F} = \frac{\int_0^\infty (C_A(t) - C_V(t))dt}{C_E} = \tau \tag{21-29}$$

where $C_A(t)$ and $C_V(t)$ are the arterial and venous concentrations as a function of time and C_E is the equilibrium concentration in the blood, usually approximated by a venous value at a selected time (e.g., 10 minutes) after the initiation of the inhalation. Typical values for this approach are τ = 2 minutes, which, from Equation 21-27 yields a flow of approximately 0.5 mL/min/g of brain tissue. A completely analogous approach with nuclear medicine imaging devices (e.g., PET and SPECT) permits one to perform these calculations regionally in the brain or other tissues and also produces estimates of blood flow using compartmental modeling approaches with a measured arterial input function and serial images of the tissue (i.e., venous efflux concentration measurements are not necessary).[6] Freely diffusible tracers used for studies of cerebral blood flow include ^{15}O-water and ^{15}O-butanol, and these are typically introduced into the body by intravenous bolus injection. Equilibrium approaches to measuring blood flow using continuous infusion of short half-life (usually ^{15}O-labeled) diffusible tracers also have been developed.[7]

One very simple method for determining the mean transit time in nuclear medicine

studies (and if the partition coefficient is known, blood flow) is the "area/height" method. A very short bolus of a freely diffusible tracer such as ^{133}Xe is injected. A gamma camera then is used to image the washout of the tracer from the organ of interest over time. It can be shown that the mean transit time is[8]

$$\frac{\lambda}{F} = \tau = \frac{\int_0^\infty A(t)dt}{A(0)} \qquad (21\text{-}30)$$

in which $A(t)$ is the amount of the tracer in tissue as a function of time after the injection and $A(0)$ is the amount of tracer in the tissue just after the bolus has been delivered. Figure 21-13 illustrates this approach graphically.

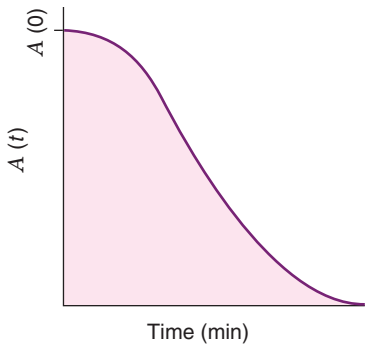

FIGURE 21-13 Tissue time-activity curve following bolus injection of a blood flow tracer. The total amount of activity detected in a given tissue region is plotted as a function of time. The maximum activity at time zero represents $A(0)$. From Equation 21-30, the mean transit time, τ, is given by the area under the curve divided by the height of the curve, $A(0)$. This method often is referred to as the "area/height" method.

5. Enzyme Kinetics: Glucose Metabolism

Enzymes catalyze many biochemical reactions that are of interest from the modeling standpoint. An example is the hexokinase-catalyzed phosphorylation of glucose that is the step initiating glycolysis and also is the focal reaction for the deoxyglucose and 2-deoxy-2[^{18}F]fluoro-D-glucose (FDG) model for determining rates of glucose metabolism (references 1 and 9). FDG is by far the most commonly used PET radiopharmaceutical in clinical studies, because many different diseases can result in changes in glucose metabolism (see Chapter 18, Section F). The model for determining the rate of glucose use from a PET study therefore is one of the most studied tracer kinetic models in nuclear medicine.

The *Michaelis-Menten* hypothesis states that an intermediate complex is formed between a reactant (also known as the *substrate*) and an enzyme. This complex then is converted to the chemical product with release of the enzyme. The reaction can be written in form similar to that for carrier-mediated transport (Equation 21-17):

$$S + E \underset{k_2}{\overset{k_1}{\rightleftarrows}} SE \overset{k_3}{\rightarrow} P + E \qquad (21\text{-}31)$$

where S is the substrate, P is the product, E is the enzyme, and k_1, k_2, and k_3 are the rate constants for the steps of the reaction process. Note that it is generally assumed that there is no reverse association of P and E; therefore no k_4 rate constant is present. However, in biologic systems there usually are separate enzymes for conversion of P back to S for additional regulation of reaction sequences.

The reaction rate R (conversion of S to P) is

$$R = \frac{V_m \times [S]}{[S] + K_m} \qquad (21\text{-}32)$$

and is known as the *Michaelis-Menten equation*. The term V_m (mg/min) is the maximum rate of the reaction, whereas K_m is the concentration of S that produces a reaction rate of one half the maximum value, as shown in Figure 21-14.

Equation 21-32 predicts that the reaction rate approaches the maximum value V_m as [S] approaches infinity. It is clear from Equation 21-32 and Figure 21-14 that the reaction rate is not a linear function of [S]; however, it still is possible to model such processes with linear tracer compartmental models because of the following relationship. If more than one substrate is competing for the enzyme E (i.e., S and S′), it can be shown[1] that the reaction rates R and R' for the competing processes are

$$R = \frac{V_m \times [S]/K_m}{([S]/K_m) + ([S']/K'_m) + 1} \qquad (21\text{-}33)$$

$$R' = \frac{V'_m \times [S']/K'_m}{([S]/K_m) + ([S']/K'_m) + 1} \qquad (21\text{-}34)$$

where V'_m and K'_m are the Michaelis-Menten constants for the reaction with substrate S′. If S′ represents a tracer of the original

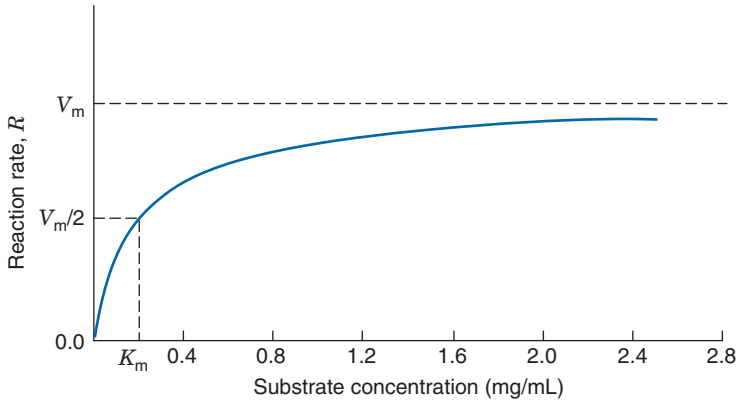

FIGURE 21-14 Graphical illustration of Michaelis-Menten enzyme kinetics. The rate of a reaction (i.e., the reaction flux R) is plotted against substrate concentration [S] using Equation 21-32. Note that when the substrate concentration equals K_m, the reaction rate is $V_m/2$. As the substrate concentration increases, the reaction rate gradually approaches V_m. (*From Phelps ME, Mazziotta JC, Schelbert HR:* Positron Emission Tomography and Autoradiography: Principles and Applications for the Brain and Heart. *New York, 1986, Raven Press.*)

substrate S, then [S′] is of a much lower value than [S]. Therefore

$$R \cong \frac{V_m \times [S]}{[S] + K_m} \qquad (21\text{-}35)$$

$$R' \cong \frac{V'_m \times K_m / K'_m}{[S] + K_m}[S'] \qquad (21\text{-}36)$$

R is simply the original rate of the process (Equation 21-32) unaffected by the presence of the tracer S′, whereas R' is a linear function of [S′] as long as [S′] remains much less than [S] (i.e., as long as the tracer condition holds). Therefore the tracer concentration [S′] is linearly related to the reaction rate R' and linear modeling techniques are appropriate for describing this process. Dividing Equation 21-36 by Equation 21-35 yields

$$\frac{R'}{R} = \frac{V'_m \times K_m [S']}{V_m \times K'_m [S]} \qquad (21\text{-}37)$$

The reaction rate of the measured or "traced" process, R', is therefore directly related to the "natural" or unknown rate R by a ratio of the Michaelis-Menten constants and the relative concentrations of S and S′. In some cases (e.g., direct isotopic substitution labeling of biologic compounds such as ^{11}C for ^{12}C), the Michaelis-Menten constants for the tracer and natural substance are essentially the same and Equation 21-37 would reduce to a simple ratio of [S′] to [S]. With analog tracers the Michaelis-Menten constants are different than the natural substance but Equation 21-37 still applies.

As an example of an analog tracer approach to modeling an enzymatic process, consider the Sokoloff deoxyglucose method[9] or the analogous approach with PET using ^{18}F-labeled FDG for measuring glucose metabolism in the brain.[10] Glucose supplies 95% to 99% of the brain's energy in normal physiologic states, and the rate of glucose use is an excellent indicator of energy-requiring functions of the brain.

FDG is an analog of glucose that is similar to glucose in several respects. Like glucose, it is transported from the blood to the brain by a carrier-mediated diffusion mechanism. Hexokinase catalyzes the phosphorylation of glucose to glucose-6-PO_4 and FDG to FDG-6-PO_4. In both the transport and phosphorylation steps, FDG is a competitive substrate with glucose. FDG-6-PO_4, however, is not a significant substrate for further metabolism. As shown in Figure 21-15, it is not converted into glycogen to any significant extent and is not further metabolized in the glycolytic pathway. The FDG-6-PO_4 also does not diffuse across cell membranes and is therefore metabolically trapped in tissues, which is convenient both from an imaging and modeling viewpoint.

If glucose metabolism in the tissue of interest is assumed to be in a steady state (i.e., it has a constant rate), then the rate of the hexokinase reaction will be the rate of the entire process of glycolysis (see Section B.6). A compartmental configuration for the FDG model is shown in Figure 21-16. The three-compartment model consists of FDG in plasma, FDG in tissue, and FDG-6-PO_4 in

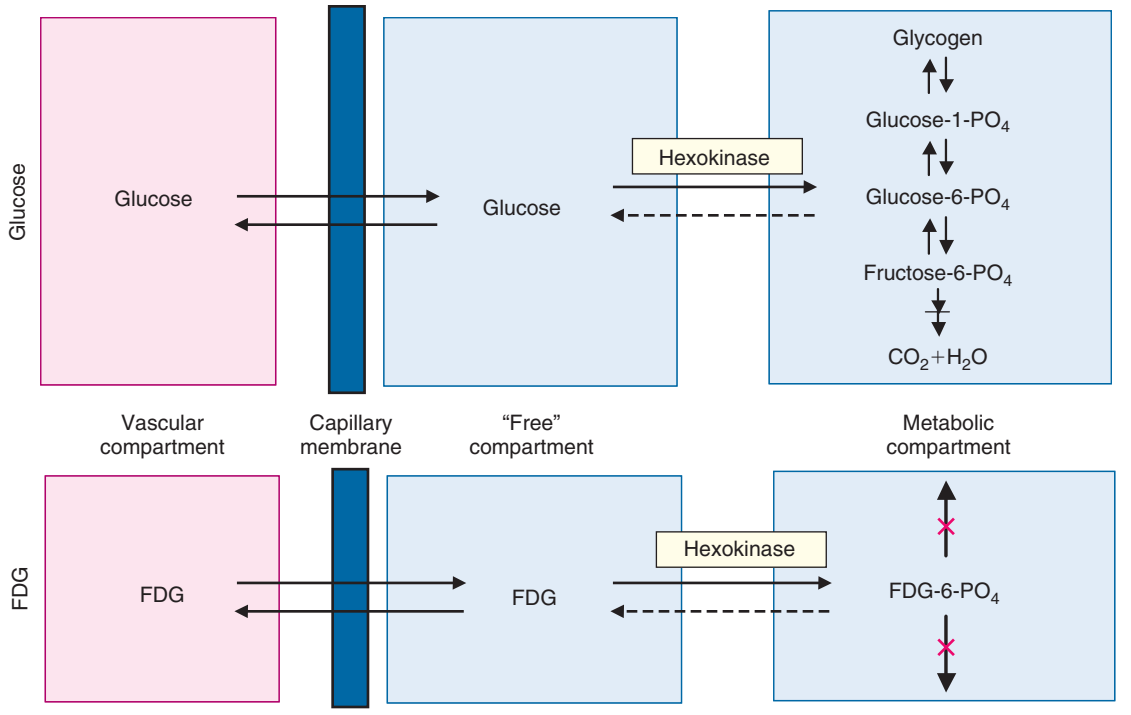

FIGURE 21-15 Transport and metabolic pathways for glucose and 2-deoxy-2[^{18}F]fluoro-D-glucose (FDG). Physically, the "free" compartment represents a combination of the interstitial space and the cytosol (the fluid component inside the cell, excluding the nucleus) in both of which unphosphorylated glucose and FDG are uniformly distributed. The red crosses indicate that FDG-6-PO$_4$, unlike glucose-6-PO$_4$, is not further metabolized.

tissue corresponding to comparable distributions of glucose, although glucose continues on through metabolism. The first-order rate constants k_1^* and k_2^* describe the transport of FDG from the blood to brain and brain to blood, respectively, whereas the first-order rate constants k_3^* and k_4^* describe the phosphorylation of FDG and dephosphorylation of FDG-6-PO$_4$. The asterisk refers to FDG indices, whereas the corresponding terms for glucose do not have an asterisk.

Let $MRGlc^*$ (μmol/min/g) refer to the metabolic rate of FDG and $MRGlc$ (μmol/min/g) be the metabolic rate for glucose. If C_t is the concentration of free (unphosphorylated) glucose in the tissue space and C_t^* is the corresponding concentration for FDG (second compartment, top row, Fig. 21-16), then, from

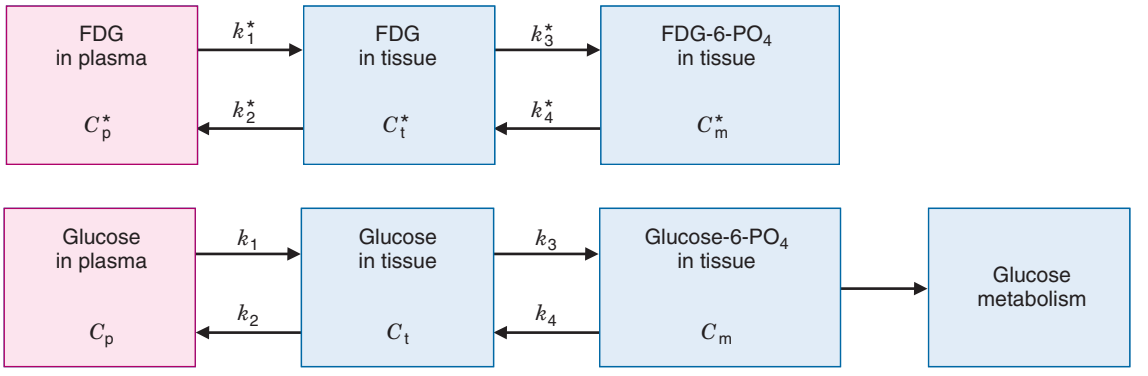

FIGURE 21-16 Three-compartment FDG model with the four first-order rate constants describing transport between the compartments. C_p, C_t, and C_m are the concentrations of glucose in plasma, tissue, and metabolized glucose (glucose-6-PO$_4$) in tissue, respectively. C_p^*, C_t^*, and C_m^* are the corresponding concentrations for FDG.

Equation 21-37 and the fact that the rate of phosphorylation (i.e., flux as described in Sections B.4 and B.5) equals $k_3 \times C_t$ for glucose and $k_3^* \times C_t^*$ for FDG, it follows that

$$\frac{MRGlc^*}{MRGlc} = \frac{V_m^* \times K_m \times C_t^*}{V_m \times K_m^* \times C_t} = \frac{k_3^* \times C_t^*}{k_3 \times C_t} \quad (21\text{-}38)$$

Equation 21-38 assumes that k_4^* and k_4 are very small and the forward rate of phosphorylation of glucose and FDG approximate the net metabolic rates. V_m and K_m are the Michaelis-Menten constants for the hexokinase-mediated phosphorylation of FDG (*) and glucose (no *).

If the ratio of terms defined by Equation 21-38 is a constant, then

$$MRGlc = MRGlc^*/\text{constant} \quad (21\text{-}39)$$

If plasma glucose (C_p) and plasma FDG (C_p^*) concentrations are constant and both sides of Equation 21-38 are multiplied by C_p/C_p^*, then

$$\frac{MRGlc^*/C_p^*}{MRGlc/C_p} = \frac{V_m^* \times K_m \times C_t^*/C_p^*}{V_m \times K_m^* \times C_t/C_p} \quad (21\text{-}40)$$

But, from Equation 21-3, the ratios C_t^*/C_p^* and C_t/C_p are the partition coefficients (i.e., tissue-to-blood concentration ratios) of FDG (λ^*) and glucose (λ). If the numerator and denominator of the left side of Equation 21-40 are divided by blood flow (F), the numerical value of the equation does not change; thus, with these substitutions,

$$\frac{MRGlc^*/(C_p^* \times F)}{MRGlc/(C_p \times F)} = \frac{V_m^* \times K_m \times \lambda^*}{V_m \times K_m^* \times \lambda} \quad (21\text{-}41)$$

This ratio of terms is defined as the *lumped constant* (LC) of the FDG model. The left side of Equation 21-41 is simply the net extraction of FDG (E_{net}^*) divided by the net (i.e., steady-state) extraction of glucose (E_{net}). Therefore,

$$LC = (E_{net}^*)/(E_{net}) \quad (21\text{-}42)$$

That is, the lumped constant of the FDG model is just the steady-state ratio of the net extraction of FDG to that of glucose at constant plasma levels of FDG and glucose. The lumped constant is a direct consequence of Equation 21-37 and illustrates the principle of competitive enzyme kinetics applied to tracer kinetic modeling. Intuitively, the lumped constant is simply a correction term that measures the net difference in the way a tissue uses FDG and glucose. The full expression of LC also includes an additional term including the influence of dephosphorylation of glucose on the net metabolic rates of FDG and glucose. This latter term is normally quite close to 1 but is intrinsically included in the measured values of LC by Equation 21-42.

Although the lumped constant describes the differences between FDG and glucose metabolism, it is actually glucose metabolism itself that is of interest physiologically. It can be shown that $MRGlc$ is given by[1]

$$MRGlc = \frac{C_p}{LC}\left(\frac{k_1^* k_3^*}{k_2^* + k_3^*}\right) \quad (21\text{-}43)$$

The term $k_1^*/(k_2^* + k_3^*)$ is the partition coefficient (λ^*) for FDG. To understand this, consider the tracer steady state when the flux of FDG into tissue is balanced by the flux out. Thus,

$$\text{flux in} = \text{flux out} \quad (21\text{-}44)$$

$$k_1^* C_p^* = k_2^* C_t^* + k_3^* C_t^* \quad (21\text{-}45)$$

$$\frac{k_1^*}{k_2^* + k_3^*} = \frac{C_t^*}{C_p^*} \quad (21\text{-}46)$$

It is apparent from Equation 21-46 that the partition coefficient, $k_1^*/(k_2^* + k_3^*)$, is simply the tissue-to-plasma concentration ratio. Because LC is the correction factor that converts the transport and phosphorylation steps measured with FDG to those for glucose, one can perform the following transformation from values for FDG to those for glucose:

$$\frac{[k_1^*/(k_2^* + k_3^*)] \times k_3^*}{LC} = [k_1/(k_2 + k_3)] \times k_3 \quad (21\text{-}47)$$

Since $k_1/(k_2 + k_3) = C_t/C_p$, the tissue concentration of glucose, C_t, can be obtained from the plasma concentration, C_p, by

$$C_p \times k_1/(k_2 + k_3) = (C_t/C_p) \times C_p = C_t \quad (21\text{-}48)$$

Thus, from the general equation for calculating fluxes (Equation 21-5),

$$MRGlc\ (\mu\text{mol/g/min}) = k_3 \times C_t \quad (21\text{-}49)$$

Equations 21-43 and 21-49 are valid only if the dephosphorylation rate is negligible compared with the rate of phosphorylation.

Models that include dephosphorylation are described in reference 1.

Equation 21-43 produces a local estimate of *MRGlc* if C_p (the steady-state plasma glucose value) is measured, if *LC* is known and if the rate constants for FDG (k_1^*, k_2^*, and k_3^*) are determined for each region of organ of interest. The equations and procedures for measuring these rate constants are given in references 1 and 10. Although this technique generates local estimates of *MRGlc*, it does require imaging the organ over time and iteratively solving for the rate constants in Equation 21-43. In actual practice, an operational equation for the FDG model usually is employed that uses predetermined population values for the FDG rate constants and requires only a single tissue measurement of the total tissue concentration of ^{18}F (^{18}FDG + ^{18}FDG-6-PO$_4$) obtained from ROI analysis of the image data. This operational equation originally was developed by Sokoloff and coworkers[9] for autoradiographically determining *MRGlc* with ^{14}C-deoxyglucose. This technique still requires knowledge of the time course of FDG input function [$C_p^*(t)$], the plasma glucose concentration C_p, the lumped constant value (*LC*), and average values of the rate constants. The Sokoloff operational equation of the deoxyglucose model, which does not include the dephosphorylation of DG-6-PO$_4$, is given by

$$MRGlc = \frac{C_i^*(T) - [k_1^* \times e^{-(k_2^*+k_3^*)T} \times \int_0^T C_p^*(t) \times e^{(k_2^*+k_3^*)t}\,dt]}{LC\left[\int_0^T \frac{C_p^*(t)}{C_p}\,dt - e^{-(k_2^*+k_3^*)T} \times \int_0^T \frac{C_p^*(t)}{C_p} \times e^{(k_2^*+k_3^*)t}\,dt\right]} \quad (21\text{-}50)$$

where $C_i^*(T)$ is the total ^{18}F tissue concentration at time *T*.

The quantities highlighted in blue in Equation 21-50 are measured in each study. Average estimates of the rate constants and *LC* obtained from separate experiments are used as a part of the routine calculation of *MRGlc* with Equation 21-50. The use of average estimates of the rate constants over the normal range of *MRGlc* values causes little error at late times (i.e., imaging 40 minutes after injection) because they appear with terms in Equation 21-50 with negative exponentials that become small when *T* becomes large.

In words, Equation 21-50 can be expressed as

$$\begin{pmatrix}\text{Regional Glucose}\\ \text{Metabolic Rate}\end{pmatrix} = \left(\frac{\text{Plasma Glucose Conc.}}{\text{Lumped Constant}}\right) \times \left[\frac{\begin{pmatrix}\text{Total } ^{18}\text{F}\\ \text{in Region}\end{pmatrix} - \begin{pmatrix}\text{Free } ^{18}\text{FDG}\\ \text{in Region}\end{pmatrix}}{\begin{pmatrix}\text{Total Net } ^{18}\text{FDG}\\ \text{Transported to the Region}\end{pmatrix}}\right] \quad (21\text{-}51)$$

The total ^{18}F minus free ^{18}FDG equals the tissue concentration of the reaction product, FDG-6-PO$_4$.

Equation 21-50 requires knowledge of the typical kinetics of the transport and phosphorylation processes to make intelligent decisions about scan duration and imaging time. Typically, approximately 40 minutes are required for the tracer to reach a near steady state in tissue after a bolus intravenous injection of FDG. A PET image usually is obtained at this time. The ROI value over the tissue or organ of interest, together with the other model parameters described earlier, is then used to calculate local values of *MRGlc*. Figure 21-17 illustrates a *parametric image* of *MRGlc* in the brain obtained using Equation 21-50 with data from an FDG PET image. A parametric image is one in which the parameter of interest (in this case *MRGlc*) is calculated on a pixel-by-pixel basis.

The FDG model contains several simplifications based on the approaches outlined in the preceding sections. The strategy of using an analog tracer effectively eliminates many alternative biochemical pathways for glucose metabolism and makes possible the simple three-compartment model. Additionally, the transport (between the first two compartments) and phosphorylation steps (between the second two compartments) represent combined steps of more complicated multistep processes. The exchange between substructures within each compartment is assumed to be rapid compared with exchange between compartments.

Even though blood flow has a major effect on tracer delivery, it is not included in the FDG model explicitly. The extraction of FDG normally is low enough (i.e., low value of $P \times S$) that the delivery of FDG has a low dependence on blood flow. In addition, the initial flow dependence on the delivery of FDG

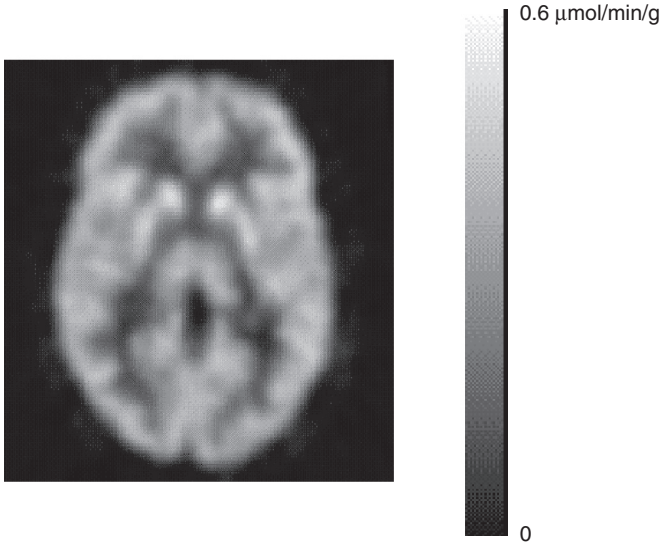

FIGURE 21-17 Parametric image of a transverse section through the brain showing *MRGlc* calculated on a pixel-by-pixel basis using Equation 21-50. (*Image courtesy Dr. Henry Huang, University of California–Los Angeles, Los Angeles, California.*)

progressively diminishes with time after injection.

In the tracer kinetic model, the FDG concentration in the vascular compartment shown in Figure 21-16 is measured by taking blood samples from the systemic circulation. Typically, it is assumed that the measured tissue data contain no significant counts from activity in the vascular space. In Equation 21-50 this is a good approximation at the typical imaging time of 40 minutes after injection. Models have been developed that add the vascular compartment to equations describing the tissue time-activity curve because in kinetic studies for measuring the rate constants, the amount of FDG in the tissue vascular pool is significant at early times after injection.

The deoxyglucose and FDG methods have been used to measure exogenous glucose use in many organs and tissues using autoradiography and PET, respectively. Examples include brain, heart, tumors, liver, kidney, and peripheral tissues.

6. Receptor Ligand Assays

Cell-surface *receptors* are important molecular targets that may be overexpressed or underexpressed in a range of important diseases states, for example in Parkinson's disease and many cancers. PET and SPECT can provide images of the distribution of these receptors by using tracers known as *radioligands* that are designed to bind specifically to the receptor of interest.[11,12] In most cases the binding is reversible, that is, over the time course of an imaging study, the radioligand and receptor are likely to disassociate. The discussion that follows assumes this case.

A simple model for the interaction of a radioligand, L, with a receptor, R, is

$$\mathrm{L} + \mathrm{R} \underset{k_{\mathrm{off}}}{\overset{k_{\mathrm{on}}}{\rightleftharpoons}} \mathrm{RL} \qquad (21\text{-}52)$$

where k_{on} and k_{off} are the rate of association and dissociation of L and R, respectively. At equilibrium, if the system is closed, there is no net change in the concentrations, and therefore

$$k_{\mathrm{on}}[\mathrm{L}][\mathrm{R}] = k_{\mathrm{off}}[\mathrm{RL}] \qquad (21\text{-}53)$$

where [L], [R], and [RL] are the equilibrium concentrations of the unbound ligand, the receptor, and the bound receptor-ligand complex, respectively. The ratio k_{off}/k_{on} is known as the *equilibrium dissociation constant* and is given the notation K_d. The total concentration of receptors is given by [R] + [RL] and is commonly denoted as B_{max}. Rearranging Equation 21-53 in terms of K_d and B_{max} yields

$$[\mathrm{RL}] = \frac{B_{\max}[\mathrm{L}]}{[\mathrm{L}] + K_{\mathrm{d}}} \qquad (21\text{-}54)$$

It is possible to measure [RL] as a function of [L] in vitro and then fit the data to estimate both K_d and B_{max}. Thus quantitative information on the receptor concentration, and the strength of binding of the ligand to the receptor (commonly known as the *affinity*, and given by $1/K_d$), can be obtained. In humans,

such a study is impractical because it would require several injections of radioligand at different concentrations. As well, at higher concentrations of the ligand there would be concerns about possible pharmacologic effects resulting from the high levels of receptor occupancy. However, if a PET or SPECT study is carried out at tracer levels such that [RL] is small compared with [R] (i.e., the fraction of receptors occupied by the ligand is, for example, 10% or less), then $B_{max} \approx [R]$, and now from Equation 21-53, we see that

$$\frac{B_{max}}{K_d} = \frac{[RL]}{[L]} \qquad (21\text{-}55)$$

The ratio B_{max}/K_d is known as the *binding potential* (*BP*) and equals the ratio of bound radioligand to free radioligand concentration at equilibrium in this simple model. Although the situation in vivo following injection of a radioligand is quite complex, it turns out with appropriate modeling of dynamically acquired PET or SPECT data that it is possible to estimate a parameter related to the in vitro *BP* as defined by Equation 21-55. Under the assumption that K_d does not change significantly with disease progression or treatment, images of *BP* will roughly reflect the relative concentration of receptors, B_{max}, in tissue. Such techniques have been widely applied to studies of receptor systems in the brain.

To see how the parameter *BP* is related to quantities that can be measured in a PET or SPECT scan, we start with a compartmental model as shown in Figure 21-18A. The injected radioligand is delivered via the flowing blood (plasma compartment) and is extracted with rate constant K_1 into the free compartment in the tissue. The rate constant K_1 represents the product of the blood flow and the unidirectional extraction fraction (see Section C.1) and has units of mL/min/g.*

*By convention, K_1 is denoted by a capital K because it has different units than the other rates constants, which are in units of inverse time.

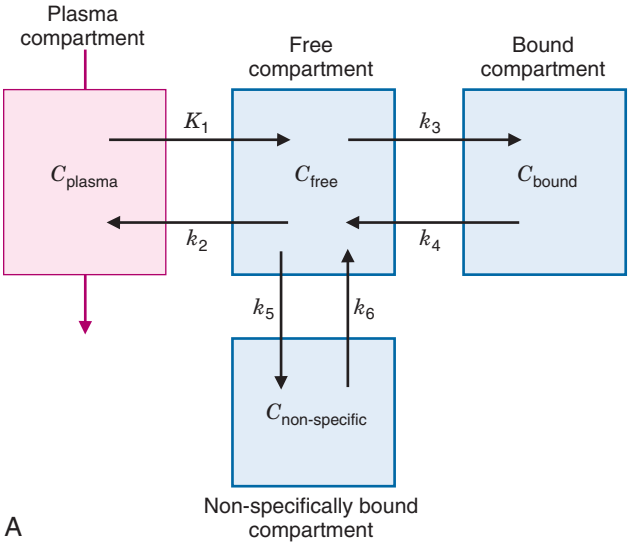

FIGURE 21-18 *A,* A general four-compartment model describing a radioligand that reversibly binds to a specific receptor. The rate constants for the exchange of the radioligand between compartments are denoted by K_1 through k_6, and the concentration of the radioligand in each compartment is denoted by *C*. *B,* A simplified version of the model in *A* in which the exchange between the "free" and "nonspecifically bound" compartments is assumed to be rapid (k_5 and $k_6 >> k_3$ and k_4) allowing these two compartments to be combined into a single compartment representing nondisplaceable radioligand. This reduces the number of model unknowns to four, increasing the robustness with which kinetic parameters can be estimated. This model is used in the analysis of many radioligand studies with PET and SPECT.

Once in the tissue, there are four possible fates for the radioligand. It can continue to exist in free form, it can bind to the receptor of interest, it can bind nonspecifically in the tissue to other proteins, or it can be transported back to the blood. Because any binding is reversible, there are rate constants both for binding of the ligand and for its dissociation. In sum, this model has four different compartments and six different rate constants.

Because of the limited temporal resolution and signal-to-noise characteristics of nuclear medicine images, it is not possible to robustly estimate six different kinetic rate constants from a dynamic PET or SPECT study. The model therefore is simplified by making the assumption that there is rapid exchange between the free and nonspecifically bound compartments, and that these two compartments can be combined together. This is a reasonable assumption if the radioligand has only low affinity binding to nonspecific targets such that it associates and dissociates rapidly (that is, k_5 and k_6 are large compared with k_3 and k_4). This combined compartment often is referred to as the *nondisplaceable compartment*. This results in the simplified kinetic model in Figure 21-18B, which consists of three compartments with four rate constants.

Based on conservation of mass, we can write simple differential equations for the concentration in the "nondisplaceable" and "specifically bound" compartments as

$$\frac{dC_{ND}(t)}{dt} = K_1 C_{plasma}(t) - k_2 C_{ND}(t) - k_3 C_{ND}(t) + k_4 C_{bound}(t) \quad (21\text{-}56)$$

$$\frac{dC_{bound}(t)}{dt} = k_3 C_{ND}(t) - k_4 C_{bound}(t) \quad (21\text{-}57)$$

At equilibrium, there would be no net transfer of radioligand between compartments; therefore, from Equation 21-57,

$$k_3 C_{ND} = k_4 C_{bound} \Rightarrow \frac{C_{bound}}{C_{ND}} = \frac{k_3}{k_4} \quad (21\text{-}58)$$

C_{bound}/C_{ND} is the ratio of the specifically bound radioligand to the radioligand in the **n**on**d**isplaceable tissue compartment at equilibrium. Thus it is closely related to the definition of the in vitro *BP* (Equation 21-55) and by convention[13] is called BP_{ND}. Examining Equation 21-56, at equilibrium, and using the relationship derived in Equation 21-58, one also obtains

$$K_1 C_{plasma}(t) + k_4 C_{bound}(t) = \frac{k_2 k_4 C_{bound}(t)}{k_3} + k_4 C_{bound}(t)$$
$$\Rightarrow \frac{C_{bound}}{C_{plasma}} = \frac{K_1 k_3}{k_2 k_4} \quad (21\text{-}59)$$

This is the ratio of the specifically bound radioligand to the radioligand concentration in **p**lasma at equilibrium. This is another form of *BP* and is given the symbol BP_P. Both definitions for *BP* can be found in the literature and only recently has consensus emerged on nomenclature.[13]

Equations 21-58 and 21-59 relate a parameter closely related to the in vitro equilibrium *BP* to kinetic rate constants that may be measured individually, or in combination, from a dynamic sequence of reconstructed PET or SPECT scans. There are several computational approaches for taking radioactivity values from such a dynamic sequence and converting them into estimates of the *BP* through the integration of Equations 21-56 and 21-57. The method used depends on the available data, for example, whether arterial blood samples were taken during the scan such that the $C_{plasma}(t)$ is known, and must also account for the fact that neither PET or SPECT can differentiate between radioactivity in C_{ND} and C_{bound}. Rather, the measurements are the sum of the radioligand in these two compartments as a function of time. Methods for computing *BP* from PET and SPECT data are reviewed in some detail in references 11 and 12. These types of approaches that integrate carefully designed radioligands, experimental protocols, and kinetic models are being used to study a number of important receptor systems, particularly in the brain (see Table 21-1). A representative example of such a study is shown in Figure 21-19.

F. SUMMARY

Tracer kinetic methods provide unique and accurate methods for measuring rates of physiologic, biochemical, and pharmacokinetic processes. This chapter has stressed some of the principles of tracer kinetic modeling in nuclear medicine and their relationship to measurements and descriptions of underlying physiologic processes. Many modeling approaches exist, and the complexity of the model that is used depends on the state of knowledge

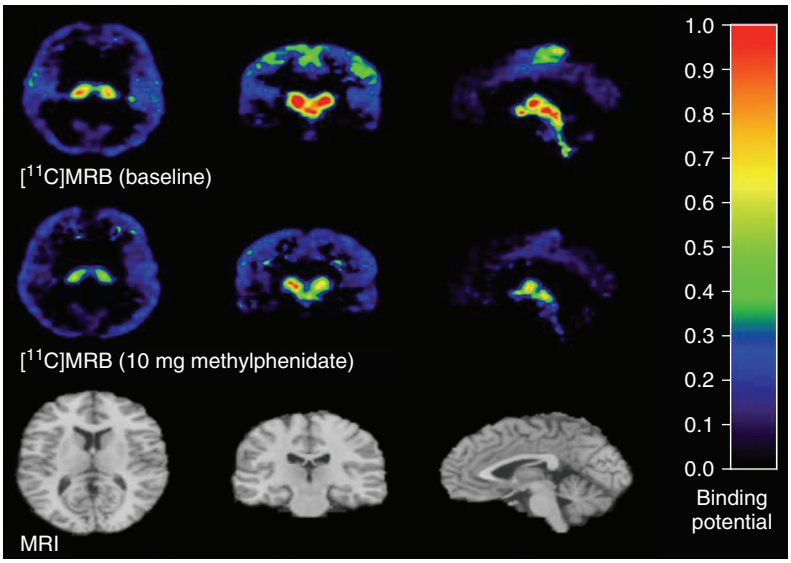

FIGURE 21-19 Images showing pixel-by-pixel calculations of binding potential (BP_{ND}) averaged over 11 healthy subjects for (S,S)-[^{11}C] methylreboxetine (MRB), a radioligand that selectively binds to the norepinephrine transporter (*top row*). This transporter is responsible for removing the neurotransmitters norepinephrine and dopamine from the synapses between neurons and is known to play an important role in several neurologic disorders, including attention deficit–hyperactivity disorder (ADHD). In this study, a decrease in binding potential was observed after administration of 10 mg of methylphenidate 75 minutes prior to radioligand injection (*middle row*). Methylphenidate is a drug that is used to treat ADHD. This study shows that methylphenidate binds to the norepinephrine transporter, thereby reducing the availability of receptor sites to which the radioligand may become bound. Sagittal, coronal, and transverse views are shown with corresponding anatomic slices from magnetic resonance imaging (*bottom row*). (*Adapted from Hannestad J, Gallezot J-D, Planeta-Wilson B, et al:* Clinically relevant doses of methylphenidate significantly occupy norepinephrine transporters in humans in vivo. Biol Psych *68:854-860, 2010.*)

regarding the fate of the tracer in a biologic system and the quality of the image data that are used as input to the model. In nuclear medicine, it rarely is possible to extract more than three or four independent parameters in a model because of the finite temporal resolution and signal-to-noise ratio of the ROI data. In situations in which the fate of the tracer is complex (multiple metabolites, multiple modes of transport, and so forth), there can be considerable debate on the appropriate formulation of the model and the exact physiologic or functional meaning of the derived parameters. Once rigorous investigative studies are carried out to validate a tracer kinetic model, it often is possible to use simplified versions of the model that provide semiquantitative indices for use in the clinical setting, where it may not be possible to acquire dynamic sequences of images or obtain blood samples.

REFERENCES

1. Gambhir SS: Quantitative assay development for PET. In Phelps ME, editor: *PET: Molecular Imaging and Its Biological Applications*, New York, 2004, Springer-Verlag, pp 125-216.
2. Renkin EM: Transport of potassium-42 from blood to tissue in isolated mammalian skeletal muscles. *Am J Physiol* 197:1205-1210, 1959.
3. Crone C: Permeability of capillaries in various organs as determined by use of the indicator diffusion method. *Acta Physiol Scand* 58:292-305, 1963.
4. Lassen NA: *Tracer Kinetic Methods in Medical Physiology*, New York, 1979, Raven Press.
5. Kety SS, Schmidt CF: The nitrous oxide method for the quantitative determination of cerebral blood flow in man: Theory, procedure, and normal values. *J Clin Invest* 27:476-483, 1948.
6. Holden JE, Gatley SJ, Hichwa RD, et al: Regional cerebral blood flow using positron emission tomographic measurements of fluoromethane kinetics. *J Nucl Med* 22:1084-1088, 1981.
7. Huang S-C, Phelps ME, Hoffman EJ, Kuhl DE: A theoretical study of quantitative flow measurements with constant infusion of short-lived isotopes. *Phys Med Biol* 24:1151-1161, 1979.
8. Zieler K: Equations for measuring blood flow by external monitoring of radioisotopes. *Circ Res* 16:309-321, 1965.
9. Sokoloff L, Reivich M, Kennedy C, et al: The [C-14] deoxyglucose method for the measurement of local cerebral glucose utilization: Theory, procedure, and normal values in the conscious and anesthetized albino rat. *J Neurochem* 28:897-916, 1977.
10. Huang SC, Phelps ME, Hoffman EJ, et al: Noninvasive determination of local cerebral metabolic rate of glucose in man. *Am J Physiol* 238:E69-E82, 1980.

11. Slifstein M, Laruelle M: Models and methods for derivation of in vivo neuroreceptor parameters with PET and SPECT reversible radiotracers. *Nucl Med Biol* 28:595-608, 2001.
12. Ichise M, Meyer J, Yonekura Y: An introduction to PET and SPECT neuroreceptor quantification models. *J Nucl Med* 42:755-763, 2001.
13. Innis RB, Cunningham VJ, Delforge J, et al: Consensus nomenclature for in vivo imaging of reversibly binding radioligands. *J Cerebr Blood Flow Metabol* 27:1533-1539, 2007.

BIBLIOGRAPHY

Additional discussion of the theory, mathematical formulation, and application of compartmental modeling, including mathematical techniques in estimation theory for modeling, can be found in the following:

Cobelli C, Foster D, Toffolo G: *Tracer Kinetics in Biomedical Research: From Data to Model*, New York, 2001, Kluwer Academic Press.